



Water Versus Land on Temperate Rocky Planets

Claire Marie Guimond¹ · Tilman Spohn² · Svetlana Berdyugina³ ·
Paul K. Byrne⁴ · Nicolas Coltice⁵ · Donald M. Glaser^{6,7} · Manasvi Lingam⁸ ·
Charles H. Lineweaver⁹ · Peter A. Cawood¹⁰

Received: 5 June 2025 / Accepted: 18 December 2025
© The Author(s) 2026

Abstract

Water and land surfaces on a planet interact in particular ways with gases in the atmosphere and with radiation from the star. These interactions define the environments that prevail on the planet, some of which may be more amenable to prebiotic chemistry, some to the evolution of more complex life. This review article covers (i) the physical conditions that determine the ratio of land to sea on a rocky planet, (ii) how this ratio would affect climatic and biologic processes, and (iii) whether future astronomical observations might constrain this ratio on exoplanets. Water can be delivered in multiple ways to a growing rocky planet — and although we may not agree on the contribution of different mechanism(s) to Earth’s bulk water, hydrated building blocks and nebular ingassing could at least in principle supply several oceans’ worth. The water that planets can sequester over eons in their solid deep mantles is limited by the water concentration at water saturation of nominally anhydrous mantle minerals, being in sum likely less than 2000 ppm of the planet mass. Water is cycled between mantle and surface through outgassing and ingassing mechanisms that, while tightly linked to tectonics, do not necessarily require plate tectonics in every case. The actual water/land ratio at a given time then emerges from the balance between the volume of surface water on the one hand, and on the other hand, the shape of the planet (its ocean basin volume) that is carved out by dynamic topography, the petrologic evolution of continents, impact cratering, and other surface-sculpting processes. By leveraging the contrast in reflectance properties of water and land surfaces, spatially resolved 2D maps of Earth-as-an-exoplanet have been retrieved from models using real Earth observations, demonstrating that water/land ratios of rocky exoplanets may be determined from data delivered by large-aperture, high-contrast imaging telescopes in the future.

1 Introduction

The world map of Earth is two thirds oceanic-blue and one third continental-brown (Fig. 1). For most of us, this map is our mental image, for better or worse, of a habitable planet. Yet studying Earth history has not clearly answered whether this condition of contemporaneous water and land has been a prerequisite for our planet’s long-term state of hosting life. The existence of billions of distant exoplanets in our Galaxy could, in principle, serve as a means to overcome this anthropic bias, although observing even a few of them in the necessary detail is one of the field’s multigenerational challenges. In the meantime, the possible existence

Extended author information available on the last page of the article

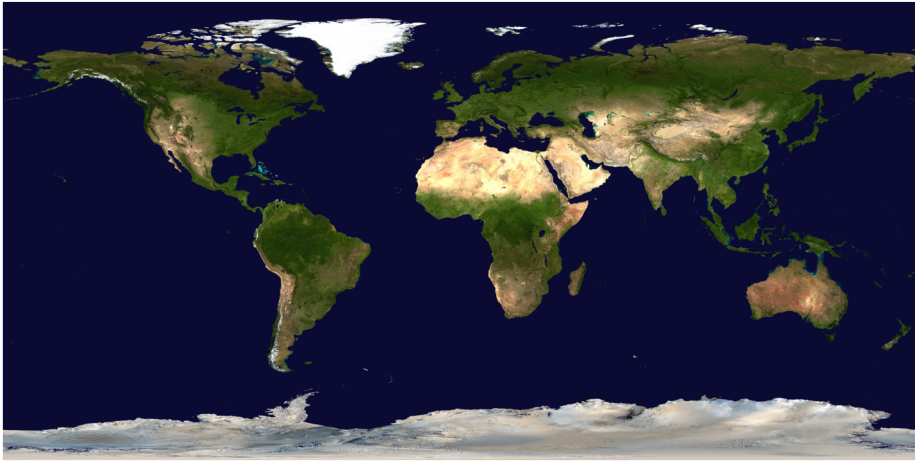


Fig. 1 Composite image of the Earth's surface compiled from NASA's Terra satellite MODIS images, with clouds removed. Credit: NASA Goddard Space Flight Center Image by Reto Stöckli (land surface, shallow water, clouds). Enhancements by Robert Simmon (ocean color, compositing, 3D globes, animation). Data and technical support: MODIS Land Group; MODIS Science Data Support Team; MODIS Atmosphere Group; MODIS Ocean Group, Public Domain, <https://commons.wikimedia.org/w/index.php?curid=50497070>

of so many rocky planets with different geological histories and bulk properties than Earth has motivated theoretical research into why — and to what extent — some planets might sustain oceans next to land, and how this ocean coverage would affect climates, biospheres, and their detectable signatures.

Working to understanding the drivers and consequences of planet surface character is in line with recent discussions of planetary ‘habitability’, going beyond stellar luminosity and atmospheric chemistry to include other planetary properties: the presence of a magnetic field, the diversity of geological provinces, and geodynamic processes such as plate tectonics that drive the interior heat engine and deep volatile cycling (e.g., Lineweaver and Chopra 2012; Heller and Armstrong 2014; Schulze-Makuch et al. 2020; Scherf et al. 2024; Stern and Gerya 2024, and see Spohn et al. 2026, this topical collection, Glaser et al. 2026, this topical collection). In the present article, we focus on the importance of ocean- versus continent-covered surface area, hereafter called the water/land ratio.

Agnostic to any future extraterrestrial life detection, such processes are also interesting for understanding how terrestrial planets evolve over time. Why does Earth have just enough liquid water on its surface to cover some, but not all, of its land? If some process(es) keep(s) Earth's oceans from either flooding the land or disappearing over billions of years, could the same process(es) be operating on other rocky planets? How do planets sculpt their crusts into continents and mountains, raising land above sea level? It is interesting to note that water, playing a fundamental role for life, has a similar fundamental role in plate tectonics. Based on their study of the evolution of continents, Campbell and Taylor (1983) wrote ‘no water, no granites — no oceans, no continents’ or as Karato (2015) put it ‘no water, no oceans, no plate tectonics, no granites, no continents’ — to which one uncertainly might add, ‘no life?’. Therefore, we ask: how does the distribution of land and oceans on a planet control its climate, and its potential to host life? Might life itself act to help regulate water cycling (Harding and Margulis 2009)? Could future astronomical observations identify water or land areas and map the surfaces of exoplanets? Although speculative, these questions are already being approached via multiple, interdisciplinary angles.

Here we consolidate the knowledge needed to start answering these questions by reviewing the growing body of work on the spatial extents of water versus land on rocky planets. First, Sect. 2.1 reviews how processes building topography carve out ocean basins, and how these mechanisms could operate across different rocky planets. Section 2.2 then provides an overview of how water is delivered to and partitioned between reservoirs inside and on the surface of the planet. Section 3 discusses some consequences of water-versus-land ratios on planetary climate and potential biospheres. Finally, Sect. 4 addresses how to detect and map water and/or land on exoplanets using future observatories.

2 Desert, Ocean, or Blue Marble: What Sets a Planet's Water/Land Ratio?

At any point in time, a planet's water/land ratio represents the trade-off between (i) the volumetric capacity of its ocean basins (e.g., Höning et al. 2014; Cowan and Abbot 2014; Höning and Spohn 2016; Simpson 2017; Höning and Spohn 2023; Dong et al. 2021; Guimond et al. 2022), and (ii) the actual volume of surface water. The volume of surface water depends on (ii.A) the total bulk inventory of water available, and (ii.B) how this water is distributed between planetary interior and surface. The volumetric capacity of the ocean basins depends on the height and distribution of topography. Section 2.1 explores point i; Sect. 2.2 explores point ii.

In sum, a rocky planet's bulk water inventory is largely set during its formation (Sect. 2.2.1), but will decrease with time due to atmospheric loss to space (see Kubyshekina et al. 2026, this topical collection). This water budget will be distributed between different reservoirs throughout the planet, the sizes of which themselves have physical limits (Sect. 2.2.2). The amount of water stored in the solid mantle cannot exceed the water solubility limits of its constituent minerals (e.g., Karato 2015; Dong et al. 2021; Shah et al. 2021; Guimond et al. 2023), which are orders of magnitude lower than the solubility of water in magma (e.g., Sossi et al. 2023). Some of the planet's water, if accreted before the segregation of its iron core, will partition into this metal and be locked there forever. At the surface,¹ the capacity of ocean basins to 'store' water is further limited by the shape of the planet's rocky surface—the volume of empty space contained below its highest point (Sect. 2.1). Excess water beyond this volume would inundate the planet's entire land mass.

Over time, the ocean volume can change according to the fluxes of water from the mantle to the surface (*outgassing*) and vice versa (*ingassing*) that control how fully each reservoir for water is filled (Sect. 2.2.2). Volcanic outgassing is a catch-all term used in this context that condenses a chain of processes. First, the convecting, volatile-bearing mantle adiabatically decompresses to create melt. Second, this melt migrates through the solid silicate interior to the surface. Third, volatiles exsolve from this melt at lower surface pressures, where they are less soluble, to ultimately produce volcanic gas. Meanwhile, ingassing can refer to a number of processes that act to bury hydrated, solid crust into the mantle. Rates of ingassing and outgassing are therefore highly dependent on the tectonic mode² of the planet

¹There is an additional reservoir for water at a planet's (sub)surface: groundwater, which we neglect given that it represents ~6 ppm of the ocean mass on Earth. Frozen surface water (glaciers and ice caps) could lock in larger fractions of the hydrosphere, and is discussed in the context of water/land ratio effects on climate in Sect. 3.1.1.

²The term *tectonic mode* encompasses the overall dynamical nature of the 'couplings' between the surface and interior (see Lenardic 2018; Stern et al. 2023).

(e.g., Kite et al. 2009; Noack et al. 2014; Komacek and Abbot 2016; Foley and Driscoll 2016; Seales and Lenardic 2020; Spaargaren et al. 2020, and see Lourenço et al. 2026, this topical collection), as well as the potential for minerals in the crust to themselves become hydrated (e.g., higher on Mars than on Earth; Wade et al. 2017; Scheller et al. 2021).

2.1 Planetary Topography and the Capacity of Ocean Basins

2.1.1 The Shape of an Active Planet: Dynamic Topography Controlled by Mantle Convection

Topography on a dynamic planet has two primary components. The isostatic component mainly reflects compositional (density) differences within the crust³ and is often conceptualised as rigid columns of rock extending above a compensation depth. This isostatic balance explains major topographic contrasts on Earth, such as the elevation differences between continents and ocean basins (see Sect. 2.1.2), and has been studied extensively for over a century. The rheological concepts of the lithosphere and asthenosphere were developed in part to explore this phenomenon (Barrell 1914).

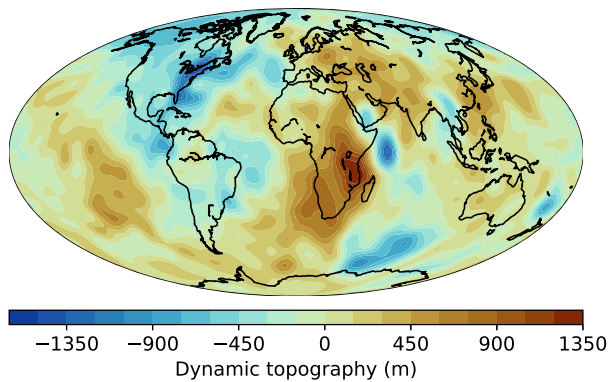
The other component arises from mantle convection and is referred to as dynamic topography (Pekeris 1935), with its global average being zero (Fig. 2). A simplistic version of dynamic topography holds that it consists of topographic highs above hot (upwelling) mantle convection currents, and lows for cold (downwelling) currents. Buoyant anomalies generate upwellings and dynamic topographic highs. For instance, the African superswell on Earth, associated with mantle plumes, corresponds to a dynamic topographic high of >500 m (Lithgow-Bertelloni and Silver 1998), whereas the margins of the Pacific, near subduction trenches, are linked to dynamic topographic lows of about 2 km (Ricard et al. 1993).

On Earth, characterising dynamic topography presents a major observational challenge because the isostatic component must be 'removed' to reveal it (see Fig. 2). The task of measuring Earth's dynamic topography is ongoing, with density models for both oceanic and continental lithospheres being developed to differentiate between the two (Hoggard et al. 2021). The challenge is even greater for Venus, where topographic observations are less precise and the tectonic mode responsible for generating internal density heterogeneities remains uncertain. However, based on long-wavelength deformation in the Baltis Vallis region, McGregor et al. (2025) suggested that dynamic topography on Venus may be lower than on Earth.

Vital clues to the origins and support mechanism of topography come in comparing spherical harmonic power spectra. Isostatic and dynamic topography generate distinct geoid signatures. On Earth, isostatically supported topography correlates well with the geoid at spherical harmonic degrees greater than 10, corresponding to shorter wavelengths (Le Stunff and Ricard 1995). In contrast, long-wavelength topography, particularly at degree 2 (corresponding to a wavelength of ~20,000 km), is generally interpreted as the surface expression of dynamic topography driven by mantle convection (Steinberger et al. 2019). Although the total topography shows poor correlation with the geoid at these long wavelengths, the predicted dynamic topography alone does correlate (Flament 2019). Notably, the spherical harmonic power spectrum of seismic anomalies in the lower mantle is also dominated by degree 2, supporting the interpretation that these anomalies reflect deep-seated density variations and associated mantle flow. Contributions at other low degrees are typically attributed to density anomalies and flow within the upper mantle (Ricard et al. 1993).

³In the Pratt model; the Airy isostasy model assumes constant crustal density but variable crustal thickness.

Fig. 2 The dynamically-supported component of Earth's topography as calculated by Straume et al. (2024), based on the SMEAN2 seismic tomography model. Data are available at <https://doi.org/10.5281/zenodo.8262689>. Note topography supported by compositional isostasy (e.g., continents), which is excluded from this map, makes up an additional component to the total topography



This observational challenge has driven the development of theoretical predictions for dynamic topography. Predictions of Earth's dynamic topography have been a subject of extensive debate and modelling (Flament et al. 2013; Davies et al. 2023). Since dynamic topography is a consequence of mantle flow, it reflects the interaction between buoyancy variations and the rheology of the deep interior. Predictive dynamic topography models are thus ultimately based on mantle buoyancy variations and rheology. The viscosity structure of the mantle influences the magnitude of dynamic topography because this structure governs how stress is distributed to deform the interfaces (Flament et al. 2013).

Both buoyancy heterogeneity and 3D viscosity result from self-organization during mantle convection. As convective vigour increases, thermal mixing intensifies, reducing the size and amplitude of thermal heterogeneities. Convective vigour and rheology are tightly interwoven with the emergent tectonic mode of a planet (Solomatov 1993; Lenardic 2018, see also Lourenço et al. 2026, this topical collection), so a key consideration in dynamic topography is the evolution of tectonic modes over time. Looking at models, however, some general patterns have become clear across the spectrum of tectonic modes:

1. If viscosity were constant throughout a planetary mantle, increasing convective vigour reduces the amplitude of dynamic topography (Bercovici et al. 1988), but leads to more rapid fluctuations. In the extreme case, as convective vigour approaches infinity, topography approaches zero. The power spectrum of dynamic topography directly reflects the dominant wavelengths of mantle flow.
2. If a planet's viscosity increases strongly with decreasing temperature, its (cold) surface may form a stagnant lid; the surface is locally too viscous to participate in convection. In such cases, plumes and small-scale instabilities beneath the viscous lid generate topography, whereas most of the mantle interior remains homogeneous. The buoyancy sources for dynamic topography are limited, and their surface expressions are filtered by the high viscosity contrast between the lid and the mantle. On a stagnant lid planet, dynamic topography amplitude still decreases with — but depends more weakly on — convective vigour, as long as there is this large viscosity contrast between the lid and mantle (Guimond et al. 2022; McGregor et al. 2025). Shorter wavelengths become more prominent in the power spectrum.
3. If viscosity also depends on stress, the planet may under some conditions enter the plate tectonics mode, with persistent subduction (Tackley 2023). In this case, again the amplitude of dynamic topography decreases with increasing convective vigour. With variable viscosity, intermediate wavelengths in the power spectrum are more pronounced than with uniform viscosity (Arnould et al. 2018). Considering the possibility of changing

tectonic modes over time, transient or extinct subduction could have left cold slabs sinking into the mantle, driving deep mantle flow and creating long-wavelength topographic lows.

4. Under scenarios involving intense melting (e.g., young and/or strongly heated planets), the planet may be described by a heat-pipe or squishy-lid tectonic mode (Moore and Webb 2013; Lourenço et al. 2020). Here, magma intrudes in the lithosphere and stalls, creating strong density variations within the lithosphere. Heat-pipe tectonics are associated with an extreme viscosity contrast between a partially molten mantle and a strong lid, resulting in dynamic topography similar to that of a stagnant lid regime. In the squishy-lid regime, the lid is softer, leading to larger dynamic topography amplitudes, particularly localized around plumes. Squishy-lid dynamics also generate transient downwellings, which could produce stronger long-wavelength components, such as those generated by deep subducting slabs today.

In summary, more-vigorous convection — i.e., at high Rayleigh number — is generally associated with lower dynamic topography amplitudes. The Rayleigh number increases with larger mantles, hotter temperatures, and lower viscosities (due themselves to hot temperatures, or high mantle water content), which for all other things being equal are expected for more massive rocky planets. Smaller, older, and colder planets with lower convective vigour should exhibit larger topographic amplitudes, influenced by the viscosity contrast between the lithosphere and mantle (Guimond et al. 2022). Meanwhile, the power spectrum of dynamic topography — its spatial distribution — is closely tied to the planet's tectonic mode. High amplitudes at low degrees are expected on planets with deep recycling of lithosphere, such as Earth's plate tectonics, with stagnant lid and squishy lid/heat pipe regimes showing shorter-wavelength dynamic topography.

With the above said, however, the topography of Mars shows that enigmatic patterns can emerge even on stagnant lid planets, due to other topographic support mechanisms beyond dynamic topography. Mars' long-wavelength topography is dominated by the isostatic component (Neumann et al. 2004). Degree 1 corresponds to the crustal dichotomy: half of Mars is thick crust in the southern hemisphere; and the other half thinner crust in the northern hemisphere. Degree 2 corresponds to Tharsis (thick crust) and Hellas annulus (thin crust). Nonetheless, there is no obvious long-wavelength dynamic topography observed on Mars.

How is a planet's water/land ratio related to its dynamic topography? For most planets, high (dynamic) topography is expected to decrease the water/land ratio by creating elevation contrasts. However, if dynamic topographic highs occur beneath isostatic topographic lows, and vice versa, the water/land ratio may increase. This situation may arise if cold convection currents (or cold structures such as slabs) occur beneath thick, buoyant lithosphere. If positive dynamic topography is concentrated in oceanic regions, the water/land ratio is maximized. Under typical scenarios, however, thick lithosphere acts as a conductive lid beneath which warmer mantle rises, either as plumes (Guillou and Jaupart 1995) or diffuse upwellings (Phillips and Coltice 2010). The actual sea level by definition follows the geoid (equal gravity-field potential): sea-level variations are expressed by the difference between the geoid and dynamic topography over continent-like areas. Nonetheless, the 3D model of Schreiber Maia et al. (2024) shows that geoid height fluctuations are small: consistently no more than 10% of the dynamic topography, across a range of mantle viscosity structures for a Venus-size planet (J. Schreiber Maia, personal communication). Hence we can view dynamic topography as a fundamental and intrinsic source of ocean basin capacity variation on geodynamically-active rocky planets.

2.1.2 Higher-Order Topography: The Evolution of Continents

Modern Earth's markedly bimodal distribution of surface elevation comes from the fact that its continents are made from lower density rock than its oceanic crust. Buoyant felsic⁴ rock, chiefly granite, dominates the continents; denser mafic rock, mainly basalt, composes the oceanic crust. Oceanic crust is produced by partial decompression melting⁵ of mantle rock beneath mid-oceanic ridges. It is returned to the mantle in subduction zones. Continental crust is produced at subduction zones (in admittedly very small net amounts in the modern era), for subduction of water, which depresses the solidus temperature, promotes partial melting of oceanic crust along with subducted sediments and mantle rock (e.g., Campbell and Taylor 1983; Stein and Ben-Avraham 2015). If the continents were more mafic and closer to oceanic crust in density, then surface elevations would be unimodally distributed. Indeed, early Archean crust before ~3.5 Ga is thought to have been more mafic, with relief correspondingly flatter (Dhuime et al. 2015; Tang et al. 2016; Cawood and Hawkesworth 2019; Chen et al. 2020; Palin et al. 2021).

Although high continental relief appears to be, unlike dynamic topography, unique to Earth, the presence of these buoyant continents is part of the key to why Earth sustains a stable intermediate water/land ratio. Some have speculated about felsic highlands on Venus (e.g., Hashimoto et al. 2008; Gilmore et al. 2015, as discussed below), for which planned Venus missions may provide substantiating data. Arguments have also been made for granitic crust forming early on Mars (McSween et al. 1999; Bandfield et al. 2004; Michalski et al. 2024; Lee et al. 2025; Malarewicz et al. 2025), as have arguments for later silica-rich igneous crust (Czarnecki et al. 2020). Apart from these still-mysterious examples, the lack of clear evidence for large-scale granitic continents beyond Earth makes it hard to predict how often we can expect them to show up elsewhere.

Still, having an understanding of why Earth's modern continental crust is on average 35–40 km thick (versus 6–7 km for oceanic crust), with a felsic composition, will give us the necessary context to thinking about any analogous hypsometric phenomenon on other planets. The detailed timing and provenance of the continents is still hotly debated (Fig. 3a; see Chowdhury et al. 2025, for a review). It is generally agreed that Earth started as a water planet (e.g., Campbell and Taylor 1983; Karato 2015; Chowdhury et al. 2025). Elevated continental land masses then evidently were seeded, rose from the seas, and grew in area over time, such that continental crust spans about 40% of Earth's surface today. Of this percentage, 87% is emerged; 13% is continental shelf covered by water. In total, 29% of the Earth's surface is subaerial land. Chowdhury et al. (2025) recently reviewed the substantial evidence for subaerial land surfaces by 3.5 Ga, although these surfaces may date back even to the Hadean (e.g., O'Neil et al. 2024). Observational constraints on the area of Earth's continental crust, and more generally on the area of its emerged land surfaces, come from the age distribution of continental crust rock (Fig. 3), the freeboard as a function of time, and geological and geochemical evidence (e.g., Cawood et al. 2022; Chowdhury et al. 2025).

Multiple lines of evidence reviewed in Cawood and Hawkesworth (2019) point to a change towards roughly modern hypsometry on Earth circa 3 Ga. The initially mafic and unimodal Archean crust is thicker than modern oceanic crust because of the hotter mantle

⁴The term 'felsic' is a portmanteau of the mineral names feldspar and silica (i.e., quartz), and refers to rocks rich in such minerals. 'Mafic' is likewise a portmanteau of 'magnesium' and 'ferric'.

⁵In partial melting of a source rock, the minerals with the lowest melting temperatures are extracted to make a new rock, leaving the minerals with the highest melting temperatures behind at the source. A reliable way to bring mantle rock above its melting temperature is adiabatic decompression upon upwelling.

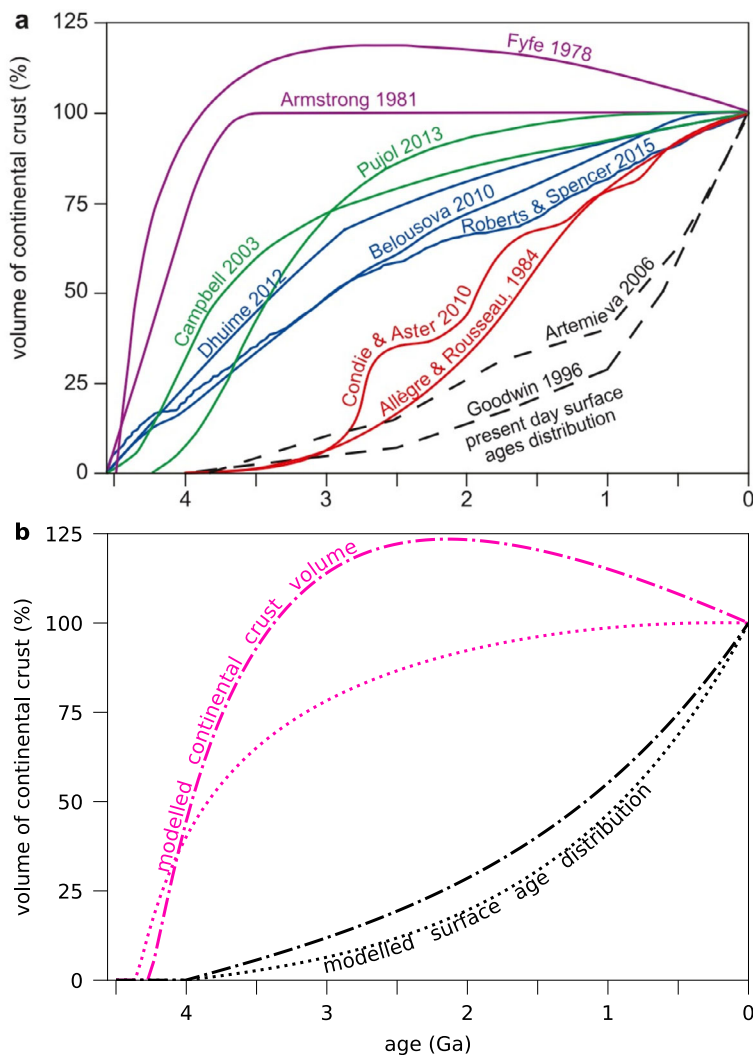


Fig. 3 (a): Models of the growth of the continental crustal volume, normalised to the present-day continental crust volume, compared with the present-day cumulative surface age distribution of Goodwin (1996). Figure adapted from Cawood et al. (2022). Note that a few more recent curves (Rosas and Korenaga 2018; Guo and Korenaga 2020) follow Armstrong (1981). (b): Continental crust growth from two models of Höning and Spohn (2023) (pink lines), compared with the same models' cumulative age distributions at the present day (black lines). Dash-dotted lines show models where 2/3 of the crustal production rate is proportional to the mantle flow velocity and 1/3 is proportional to the continent surface area; dotted lines show the reverse. All models consider thermal blanketing by continents and partitioning of heat-producing radiogenic elements into the crust. The cumulative surface age distributions are similar despite the substantially different growth curves, due to continuous production and recycling of the crust (see also Korenaga 2021b)

temperature and associated degree of melting. Melting of metamorphosed mafic rock at the base of the crust (e.g., amphibolite) could have produced the granitic rock characteristic to the Archean (tonalite–trondhjemite–granodiorite or TTG). The crust first begins to increase in both thickness and overall silica content with the emplacement of TTGs: the increasing

variability of certain geochemical tracers in the rock record around 3 Ga suggests a corresponding deviation from unimodality in crust thickness and hence hypsometry (Moyen and Laurent 2018). With the transition to plate tectonics, melting at convergent oceanic plate boundaries started to produce new crust with an average composition of (felsic) calc-alkaline andesite (Rudnick and Gao 2003), possibly establishing the thick continents in the long term.

Although associating the timing of modern hypsometry with the timing of plate tectonics is certainly tempting, debate about the connections between plate tectonics initiation and continental evolution persists in part because the rock record becomes increasingly sparse going back in time. It is widely accepted that plate tectonics has been operating through the Proterozoic, since about 2.5 Ga at the latest. Yet the beginnings of emerged land and proto-continents would have been seeded in the Archean (e.g., Cawood et al. 2013, 2022; Chowdhury et al. 2025; Frost and Mueller 2024).

The advent of plate tectonics may have also stabilised Earth's continental area due to several potential feedback mechanisms: between plate boundary type and new crust composition and/or between continental area and lithospheric stress, for example (e.g., Lenardic et al. 2005; Höning and Spohn 2016; Cawood and Hawkesworth 2019). The observed cumulative age distribution of continental crust (Fig. 3b) can be reproduced in models which assume some form of continuous continental crust production and recycling occurring through the Archean, or even the Hadean. Höning and Spohn (2023) modelled the crust production rate as proportional to the vigour of mantle convection, and the recycling rate as proportional to the area of continental crust. Under this formulation, continental growth rates would decrease with time as the mantle cools and convects less vigorously, whereas recycling rates would increase with time: rapid early crust formation that turns into a steady-state (Fyfe 1978; Armstrong 1981; Rosas and Korenaga 2018; Guo and Korenaga 2020, see Fig. 3b). Yet different assumptions about the extents of these proportionalities can result in the same cumulative growth curve, despite the actual areal growth curves differing considerably (Fig. 3b). In sum — and as reviewed in Korenaga (2021b) — definitive interpretations of the evidence remain elusive.

So is Earth's continental surface area of 40% a determined outcome of plate tectonics? Simpson (2017) used Bayesian statistics to argue that Earth should be on the dry tail of a mostly water-rich distribution. The statistical argument could be invalidated if geological feedback mechanisms stabilize a water/land ratio close to unity. In a series of papers and contemporaneous with similar efforts (Cowan and Abbot 2014; Schaefer and Sasselov 2015; Komacek and Abbot 2016), Höning and co-workers modelled water/land ratio outcomes considering plate tectonics-related feedback mechanisms in the Earth continental crust and water cycles (Höning et al. 2014; Höning and Spohn 2016, 2023). These authors concluded that the cycle would tend to either maximize the continental (land) surface area covering almost the entire planet, or maximize the area of the ocean floor (thereby minimizing the land surface), but that a balanced distribution — as on Earth — is a comparatively rare outcome (see Sect. 2.2.2). The present Earth state would be marginally stable, perhaps kinetically stabilized by the decreasing mantle temperature, but would maximize continental crust-related geodynamic activity. Meanwhile, in the absence of any mechanisms regulating ocean volume (see Karato et al. 2020), there is no reason to expect that sea level remain below peak topography (Guimond et al. 2022).

In summary, this picture of continental evolution raises the intriguing question of which if any components are inseparable from, and unique to, Earth's geodynamic history. Plate tectonics certainly set the thickness of Earth's continents, and may have stabilised their surface area (e.g., Lenardic et al. 2005; Höning and Spohn 2016; Cawood and Hawkesworth

2019; Cawood et al. 2022). However, the relevant condition to forming TTGs in the Archean may be described as bringing hydrated crust to depth, and this effect could potentially be achieved through other mechanisms, such as delamination (e.g., Sizova et al. 2015). Further, there exists evidence for land having emerged above sea level well before the accepted minimum age of subduction initiation (Chowdhury et al. 2025). The striking implication of these ideas is that at least relatively modest volumes of felsic, buoyant landmasses on a planet may not necessarily require plate tectonics to form, although they may need water.

In need of more clues, we return to the reputed ‘continental analogues’ of our nearest planetary neighbour. It is worth pointing out that the enigmatic tessera terrain-covered highlands on Venus, which morphologically, geodynamically, and perhaps even compositionally bear a strong resemblance to Earth’s cratons (Hashimoto et al. 2008; Gilmore et al. 2015) cover about 7% of the surface of Venus (Ivanov and Head 2011). Whether Venus’ tessera-covered highlands truly are counterparts to the continental cores on Earth remains an open question, and may depend on any deep water cycle. Although at first glance, the tesserae and the cratons have similar areal extents today—the felsic continental interiors on Earth, the cratons, now occupy about 8% of Earth’s surface (Hasterok et al. 2022)—whether there should be any significance to this fact is unclear, given that the margins of cratons are either structural (i.e., faulted) or covered by younger basins, implying that cratons had a greater extent in the past (e.g., Begg et al. 2009). Further, Venus’ hypsometry is unimodal, without Earth’s dichotomous elevations of oceanic and continental crust. Even so, the fact that there are highlands on Venus at all when the majority of the surface lies within only a few hundred metres of the mean planetary radius (Pettengill et al. 1980) means that, were there ever liquid water oceans on the planet (of a similar volume to Earth’s), and assuming those highlands were present in at least comparable surface area to today, they would constitute ‘dry land’ in a manner analogous to the subaerial continents on Earth.

2.1.3 Other Forms of Topography

There are additional mechanisms that can shape a planet’s topography and thus, depending on the available liquid water volume at the surface, govern the water/land ratio. For example, large-scale tectonic processes, which principally manifest on Earth as vast lateral displacements, can have a vertical component of deformation, too. This process — and especially the maximum achievable elevation — is strongly controlled by the rheological properties of the lithosphere. Only cold, mechanically strong lithospheres can support high mountains or large volcanic edifices isostatically; in contrast, hot lithospheres deform and flow under such loads (Rey and Coltice 2008). This rule is exemplified by the Voyager-era debate as to how such high mountains could exist on Io given observations of its high surface heat flow (implying a thin lithosphere under conduction). The seeming contradiction led O’Reilly and Davies (1981) to suggest that Io’s internal heat is transported by magma advection, thus giving rise to the heat-pipe theory.

Major thrust faults, formed through horizontal shortening and thickening of the crust, can readily generate topography several hundred to a few thousand meters in relief. On Earth, such thrust-fault systems are usually the result of tectonic plate convergence, forming complex thrust fault duplexes that are eroded into the familiar orogenic belts we recognize as the Alps, the Himalaya, and so on. Yet on Mercury, major thrust-fault systems standing ~2–3 km high and extending hundreds or even thousands of kilometres in length cross the planet (Byrne et al. 2014), the result of secular cooling of the planet’s interior that causes the solid planet to contract (Solomon 1977; Tosi et al. 2013). Absent plate tectonics, large-scale crustal shortening remains possible—not to the extent on a stagnant lid world as on

Earth, certainly, but enough to generate positive topography (and, by implication, spatial topographic variations in which water could pond as lakes or seas).

Whereas tectonic shortening of the crust produces positive relief, tectonic extension can similarly produce dramatic changes to the landscape, in the form of negative-relief topography. On Earth, the formation of (often vast) rift zones by tectonic plate divergence characterises seafloor spreading centres, but also occurs in continental settings; for example, within eastern Africa (cf. Fig. 2) and the southwestern United States. Some of these rift zones can have substantial negative relief (exceeding 1 km in the Basin and Range, USA), and considerable breadth (several tens of km in the case of the East African Rift). The driving mechanism for major rifting on Earth is plate tectonics, but crustal rifting is present on Venus and Mars, too (Anderson et al. 2001; Ivanov and Head 2011; Byrne et al. 2020). On these worlds, the driving apart of the crust is likely the result of mantle upwellings and/or intrusive volcanic complexes under the stagnant lid tectonic mode — with the Tharsis Rise on Mars, for example, having been explained by its underlying mantle superplume (or more recently, transient plumes; Cheng et al. 2024). Here, extension is not balanced by subduction but possibly by crustal thickening elsewhere, and so the total extensional strains are (much) lower than on Earth. Even so, topographic changes resulting from crustal rifting can be considerable.

Another non-tectonic mechanism, and one that operates widely on Earth albeit at relatively small spatial scales, is the formation of negative topography by karstic processes. Broadly speaking, karstic landscapes result from the chemical dissolution of soluble materials (chiefly limestone on Earth) by water, which takes advantage of existing fractures and other weaknesses in the crust. Karst occurs in a wide range of settings on Earth, and is characterised by the formation of often striking topography that includes towers, ridges, caves, and sinkholes — the latter of which are frequently filled with water — symbolised notably in the landscape around Guilin, China, for example. Karstic terrains have also been identified on Saturn's giant moon Titan, which in the present hosts voluminous deposits of liquid hydrocarbons that have presumably acted to erode the icy surface and subsurface in a manner akin to acidic water in carbonate settings on Earth (e.g., Malaska et al. 2020). Whether karstic process can operate on silicate exoplanets depends in great part on the composition (and solubility) of the crust, although carbonate rocks are not strictly necessary (Ford and Williams 2013), and of course on the availability of liquid water at the surface. Nonetheless, as a means to generate low-lying topography into which water can pond, karstic processes bear inclusion here.

The karstic processes described above, insofar as they create 'negative topography', might be grouped into the broader process of erosion. Although erosion's net effect, over 100-Myr timescales, is to grind down mountains, on shorter time scales at which the elastic bending of the lithosphere and isostatic adjustment are relevant, erosion has complex effects on subcontinent-scale topography (e.g., Wolf et al. 2022). Physically removing mass — erosional unloading — through the action of glaciers, to exemplify the most important erosive agent on Earth (Dowdeswell et al. 2010) — can cause uplift of the lithosphere locally as it rebounds (e.g., Champagnac et al. 2009; Liu et al. 2024). The continents of a planet with glacial-interglacial cycles would bear the scars of glacier motion. Though the characteristic geomorphological features (e.g., drumlins, kettle lakes) are relatively short or shallow, they would be widespread, again guaranteeing the ubiquity of 'little ponds'.

The processes discussed here are internally driven and reflect some interplay between the thermal evolution of the body, the convective vigour of the interior, and the mechanical strength (and composition) of the brittle lithosphere. Yet arguably the most effective mechanism for shaping a planet's topography is not internal at all. Impact bombardment

has the demonstrated ability to dramatically alter a planetary body's landscape at all scales by excavating and redistributing crustal (and mantle) materials to form topographic lows and highs, often adjacent to one another, and thus creating undulating topography in which water could pond as lakes, seas, or even oceans. For example, at the very largest scales, impact cratering is responsible for the lunar South Pole–Aitken basin, the largest impact feature on the Moon (e.g., Zuber et al. 1994); the mighty Caloris basin on Mercury (Murchie et al. 2008); Mars' huge Hellas, Argyre, and Isidis basins (e.g., Schultz and Frey 1990); and even, perhaps, the Red Planet's vast northern lowlands (e.g., Wilhelms and Squyres 1984; Andrews-Hanna et al. 2008). Indeed, exogenous causes for the famous martian hemispheric dichotomy largely rely on one or more impacts so energetic as to have excavated and/or melted a large fraction of the surface. More recent explanations argue that although the lowlands are not an impact basin, the highlands are the result of crystallising a giant impact-induced magma pond in the south (Reese et al. 2011; Golabek et al. 2011; Cheng et al. 2024). Although the past presence of an expansive northern ocean on Mars continues to be debated (Baker et al. 1991; Malin and Edgett 1999; Perron et al. 2007; Schmidt et al. 2022; Wu et al. 2024; Li et al. 2025), there is little question that *were* liquid water to exist on the surface in sufficient volumes to constitute a sea or even ocean, that water would certainly pond in the northern lowlands.

Far more certain is the ponding of liquid water in Mars' smaller impact features, evinced by the lacustrine sedimentary deposits in Gale (Edgar et al. 2020) and Jezero (Goudge et al. 2015) craters, the field sites of the robotic Curiosity and Perseverance geologists, respectively. These craters are much smaller in size (~50–150 km wide) than the giant basins listed above (which all exceed 1500 km in diameter), and so could much more readily host standing bodies of water of even modest volume. Of note, impact features (on rocky worlds) can be isostatically compensated and so do not require dynamic support from below to form or be sustained, with even the very largest basins being supported by membrane stresses,⁶ and thus these features can persist over geological time. Viscous relaxation of the crater form on icy worlds is well documented (e.g., Parmentier and Head 1981), but much less so on silicate bodies.

There are clearly no shortage of processes that can generate variations in topography that deviate from some mean, thus allowing the ponding of water into lakes, seas, or even oceans—assuming such water volume is present. On the basis of what we see in the Solar System, it seems to be far more probable to produce and sustain high- and low-standing topography than it is to form and hold onto an ocean. Whether that is the case for extrasolar worlds is discussed below.

2.2 Planetary Surface Water Inventories

2.2.1 Estimating Planetary Bulk Water Budgets

In practice, inferences about an exoplanet's mass fraction of highly volatile materials (water and ices, e.g.) can come from its measured bulk density because volatiles are less dense than rock and iron (see Baumeister et al. 2025, this topical collection, for an extensive discussion). For those planets *less* dense than rock and iron, a substantial fraction of light material is required to make up the density deficit. However, even if we could know that this light component were water in condensed form on the surface of the planet, the amount of water required to make an Earth-mass planet measurably less dense (i.e., by 0.3 g cm^{-3} by

⁶That is, stresses that are uniform with depth in the lithosphere, which behaves elastically.

analogy to the TRAPPIST-1 system; Agol et al. 2021) is about 2–3% of the planet mass, or 180–250 km deep, for example.⁷ This volume of water would necessarily result in an ocean-covered world, as it well exceeds the supportable topography (Guimond et al. 2022). Even wielding infinitely-precise measurements, larger ocean masses could be masked by a larger bulk iron content, absent degeneracy-breaking prior knowledge (such as a hot equilibrium temperature⁸ precluding surface oceans or ice). Therefore, although bulk density observations may identify distinctly volatile-rich planets as such (Baumeister et al. 2025, this topical collection), we do not expect to be able to use this technique to infer the ocean mass fraction of a potentially ‘blue marble’ planet.

The plausible water budgets of cool, potentially-rocky planets could be informed instead by theory encompassing planet formation, metal-silicate differentiation (i.e., segregation of H and O into a metal core), and irreversible loss of the atmosphere to space (on the latter, see Kubyshkina et al. 2026, this topical collection). To first order, whether the main building blocks of a planet originate outside or inside the snow line in a protoplanetary disk (corresponding to the temperature below which water condenses) controls whether this planet likely forms with large ($\gg 1$ wt.%) or small ($\ll 1$ wt.%) water mass fractions (e.g., Tian and Ida 2015; Lichtenberg et al. 2021). In detail, however, the complexities and stochastic nature of the aforementioned processes — as well as others not considered here, such as orbital migration — mean that predicting the precise water inventory of an exoplanet inside the snow line is likely to be impossible.

Nonetheless, there are a number of potential, non-mutually-exclusive sources of water to the growing Earth and other planets inside their disk’s snow line:

1. *Wet accretion*: The primitive building blocks of planets may themselves contain some fraction of hydrogen by mass. In the inner regions of the Solar System, these building blocks may be represented by enstatite chondrites (Javoy 1995). Although previously thought to be dry, recent measurements by Barrett et al. (2025) have shown that enstatite chondrites do contain H bound to S, enough to supply up to 10 ocean masses⁹ from 1 Earth mass of building blocks. In addition to the enstatite chondrite contribution, carbonaceous chondrite material from the wetter, outer Solar System could make up ~ 2 –5% of Earth’s mass, corresponding to several oceans (based on Xe isotopes; Cassata 2025). A potential issue with accreting planetary water from undifferentiated chondrites is that these building blocks would have not experienced much heating; else they would have differentiated, degassing water in the process. More strongly-heated protoplanets would make drier planets (Lichtenberg et al. 2019; Sanderson et al. 2024).
2. *Late(r) accretion*: After the bulk of the planet’s mass has accreted and differentiated, water is delivered to its surface via impacting material scattered in from beyond the snow line (e.g., Morbidelli et al. 2000; Hartogh et al. 2011; Alexander et al. 2012; Marty 2012; Mandt et al. 2024). Isotope constraints point to at least some contribution to the bulk Earth from outer Solar System material (e.g., Burkhardt et al. 2021, although the exact contributions remain unresolved). The important distinction between this process and

⁷If this water were instead dissolved in a fully-molten mantle of a young, hot planet, an even higher water mass fraction would be required to affect the bulk density signature (Dorn and Lichtenberg 2021; Luo et al. 2024). A *solid* mantle is unlikely to be able to store enough water to increase its radius beyond the observational uncertainty, given lower water concentrations at water saturation (Shah et al. 2021).

⁸The equilibrium temperature of a planet is the temperature at which it radiates away all of the stellar energy it receives, less a nominal fraction reflected. The presence of greenhouse gases would raise the actual surface temperature above this equilibrium temperature.

⁹An ocean mass amounts to about 1.34×10^{21} kg, equivalent to 333 wt. ppm of the bulk silicate Earth.

the one above is that the cumulative water delivered through smaller impacts depends on highly-stochastic dynamical scattering, sensitive to, for example, the migration history of the giant planets (Raymond et al. 2004). Meanwhile, accreting water at this post-differentiation stage guarantees that such delivered water is not permanently sealed in an iron-alloy core.

3. *Nebular ingassing*: Hydrogen gas of stellar nebular origin,¹⁰ upon reacting with a primordial magma ocean, could be oxidised to produce water if it lingers long enough (Ikoma and Genda 2006; Sharp et al. 2013; Sharp 2017; Olson and Sharp 2018, 2019; Kimura and Ikoma 2020; Kite and Schaefer 2021; Kimura and Ikoma 2022; Young et al. 2023; Krissansen-Totton et al. 2024). For example, Olson and Sharp (2019) estimated that, in theory, Earth could have acquired and retained at least an oceans' worth of water through nebular ingassing alone. This estimate would be lower for a less-oxidising magma ocean; in this way such nebular water production is also tied to the relative timing of core formation.
4. *Direct accretion of H₂O vapour*: Water-bearing material drifting inward across the snow line could sublimate, whereupon the water vapour viscously diffuses under the influence of a growing planet's gravity (Kral et al. 2024; Houge et al. 2025).

The Bulk Water Budget at Birth In sum, the multitude of processes that might deliver and/or make available water to inner regions of protoplanetary disks suggests that it need not be difficult for some rocky planets to gain rather substantial initial water inventories. Meanwhile, planetary differentiation ensues; possibly-large fractions of hydrogen partition into the metal that initially separates from silicate material (hydrogen favours metallic melt over silicate melt at terrestrial planet core-formation pressures; e.g., Okuchi 1997; Li et al. 2020; Tagawa et al. 2021; Luo et al. 2024; Liu and Jing 2024). This water equivalent probably becomes locked in the core forever.¹¹ As for the remaining water, we now believe water to be highly soluble in primordial magma oceans, even miscible above a few GPa, such that (temporary) sequestration of this water is quite feasible (e.g., Bureau and Kepler 1999; Mibe et al. 2007; Dorn and Lichtenberg 2021; Bower et al. 2022; Sossi et al. 2023).

It then becomes a different question of whether the bulk silicate planet's water can be retained through the early evolution of the planet. Answers to the water retention question are tied to the duration of a primordial magma ocean and its trade-off with the timing of escape of hydrogen from the upper atmosphere (e.g., Zahnle et al. 1988; Lebrun et al. 2013; Hamano et al. 2013; Miyazaki and Korenaga 2022a), subject further to unpredictable catastrophic events such as giant impacts (e.g., Biersteker and Schlichting 2020; Saurety et al. 2025). On the one hand, a long-enduring magma ocean, continuously degassing volatiles,¹² would be exposing more water vapour to extreme UV radiation from the host star (Hamano

¹⁰Whereas there is no direct evidence of an enduring primordial hydrogen atmosphere on Earth, it has been proposed that many observed rocky exoplanets today are the remnants of initially more gas-rich planets that have lost their hydrogen atmospheres (Owen et al. 2020). However, since the photoevaporative process that removes hydrogen would work less efficiently on cooler planets, it remains to be seen whether more-temperate rocky exoplanets have experienced something similar.

¹¹The core is potentially the largest H reservoir in the interior of the Earth; 51 oceans-worth of hydrogen have recently been proposed by Liu and Jing (2024). Water 'locking' in the core is helped by the small diffusivity of H in lower mantle rock.

¹²In magma ocean models, the degassing rate of water from the magma surface is typically controlled by a vapour pressure equilibrium (Henry's Law). If atmospheric escape drives the partial pressure of water to continuously decrease, more water will be continuously degassed to maintain equilibrium, barring some other bottleneck to degassing (such as in Salvador and Samuel 2023; Walbecq et al. 2025).

et al. 2013; Kite and Barnett 2020; Salvador et al. 2023). On the other hand, the very high potential of magma to hold water means that, *for as long as this magma ocean has not mostly solidified*, it could easily be protecting many ocean-masses of water from such radiation (Dorn and Lichtenberg 2021; Bower et al. 2022; Sossi et al. 2023; Moore et al. 2023; Nicholls et al. 2024; Maurice et al. 2024). As the magma ocean cools and crystallises, the capacity of the mantle reservoir markedly decreases because water is much less soluble in silicate *crystals* compared with melt (see Sect. 2.2.2). The inevitable decrease in reservoir capacity implies that a large fraction of water must go somewhere else, presumably above-ground (e.g., Tikoo and Elkins-Tanton 2017; Krissansen-Totton and Fortney 2022; Miyazaki and Korenaga 2022a; Salvador et al. 2023), by which time the star may or may not have become less active. In any case barring total dessication, the newly-crystallised mantle rock still traps some of the magma ocean's hydrogen according to its finite solubility in this rock, as could any interstitial melt (Tikoo and Elkins-Tanton 2017; Miyazaki and Korenaga 2022a,b; Salvador et al. 2023; Lu et al. 2025). Thus there are potential avenues for at least *some* internal water retention even after the magma ocean phase effectively ends.

Massive water losses do seem particularly hard to avoid for planets on close-in orbits around M-dwarfs — i.e., most of the best-observed rocky exoplanets to date — given inferred high rates of atmospheric escape even to the present (see Kubyshkina et al. 2026, this topical collection). Nevertheless, astronomers are seeking to empirically test the retention of volatiles on rocky planets by looking for signs of atmospheres (see Lustig-Yaeger et al. 2026, this topical collection).

Do we expect a young planet's hydrosphere to condense as oceans? Water not containable in the mantle may be quickly degassed as steam. This steam condenses if the surface and atmosphere can sufficiently cool down, implying that greenhouse gases such as CO₂ must not be *too* abundant (e.g., Salvador et al. 2017, 2023; Miyazaki and Korenaga 2022a), whereas star-planet distance (planetary insolation) may play a key role (Turbet et al. 2021). Conditions were evidently met on early Earth (e.g., Mojzsis et al. 2001), but the same is not obvious for all planets, as exemplified in the active debate around an early temperate phase on Venus (e.g., Way et al. 2020; Turbet et al. 2021; Westall et al. 2023b).¹³

2.2.2 The Deep Water Cycle: Geodynamics and Mineralogy

A planetary body's bulk water content is mostly set during its formation, but the distribution of water between the surface and the interior can vary between planets and in time (e.g., Williams 2007; Karato 2015; Salvador et al. 2017; Miyazaki and Korenaga 2022a). As the previous section suggested, water is feasibly present inside the body from its early stages. Given billions of years, this interior water reservoir is carried through the mantle as it convects, and could slowly empty to the surface through subsequent melting and volcanic outgassing. The action of plate tectonics changes the loci of outgassing, but volcanism in the first place does not require plate tectonics (Fig. 4). Phenomena analogous to Earth's hotspot volcanoes (e.g., Hawai'i) are evidenced by Olympus Mons (and major plains volcanism on all single-plate worlds).

Less certain is the ubiquity of water ingassing to the mantle. On modern Earth, the ingassing mechanism takes the form of subduction of crust containing hydrated minerals, so Earth's deep water cycle is completed (e.g., Jacobsen and van der Lee 2006; Rüpke and Gaillard 2024, compare Fig. 4). About 10¹² kg of water enters Earth's subduction zones

¹³Although this review does not cover how and when plate tectonics can initiate, we note that ocean condensation is probably important (e.g., Miyazaki and Korenaga 2022b).

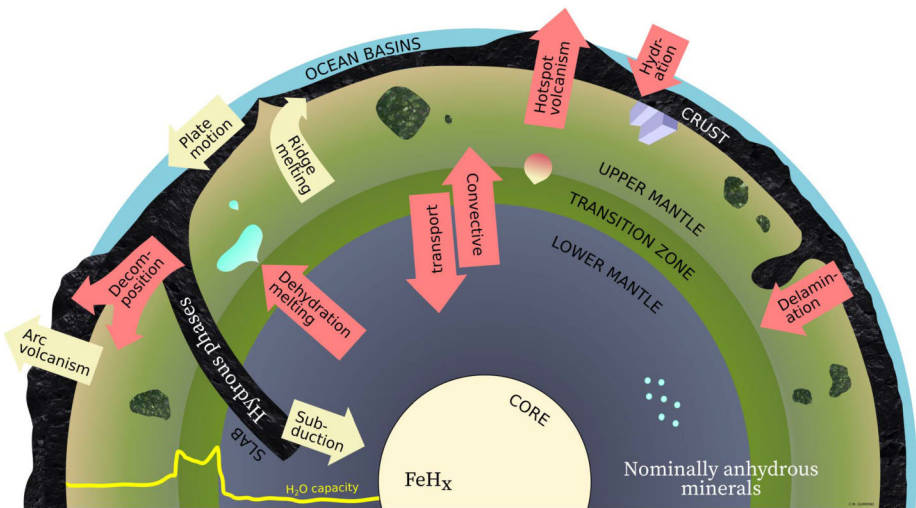


Fig. 4 Elements of the deep water cycle on rocky planets that are discussed in this article. Reservoirs are labelled in sans serif font. The dominant form of ‘water’ in certain reservoirs is noted in serif font. The major fluxes potentially possible on rocky planets in general are marked in red arrows, whereas the fluxes operating only under plate tectonics are marked in yellow arrows. The profile in the bottom left corner indicates the relative water concentration at water saturation in nominally anhydrous minerals for an Earth-like mantle composition. Note geometry is not to scale

each year, largely as hydrous minerals and pore water in sediments and hydrated basaltic crust (Karato 2015, and references therein). Indeed, Earth is believed to have been in a state of net water ingassing to the mantle for a large part of its history (e.g., Ito et al. 1983; Jarrard 2003; Van Keken et al. 2011; Karlsen et al. 2019; Korenaga 2021a, and references therein). The geological record suggests an intriguingly constant freeboard (or, sea level) during the last ~500 Myr (e.g., Parai and Mukhopadhyay 2012), perhaps hinting at a feedback mechanism at play.

We can look to the Solar System for clues about water ingassing under other tectonic modes. There are no active subduction zones on Mars, but some ingassing mechanism is not ruled out completely. Petrologic modelling suggests that Mars’ small size and iron-rich crust could allow that crust, upon hydration (consuming surface liquid water), to remain dense enough to remain buried under new volcanic lava flows, eventually sinking to the upper mantle, bringing hydrated minerals with it (Wade et al. 2017). Although little about Venus’ water cycle is known, evidence for compositionally-diverse lava indicates some amount of heterogeneous processing, perhaps mediated by volatiles. Hence Elkins-Tanton et al. (2007) demonstrated with a geodynamic model that gravitational instabilities could drag parts of a volatile-bearing lithosphere back to the upper mantle in this scenario. It should be noted that in reality, so-called tectonic modes (hence available ingassing mechanisms) need not be neat nor permanent (Lenardic 2018). For example, water may be returned to the mantle during an episode of resurfacing for an otherwise fairly immobile lithosphere (e.g., Vezinet et al. 2025).

Ingassing is important because in its absence, and given some degree of outgassing, a temperate planet’s ocean volume would always increase with time, barring rapid atmospheric escape (or impact blowoff) or a climate catastrophe. Some planets may also have limited-to-no outgassing — hence no flux of water at all — if wet buoyant magma does not

form under a very thick lithosphere, as predicted for more massive rocky planets without plate tectonics (Kite et al. 2009; Dorn et al. 2018; Ortenzi et al. 2020).

Water Capacities of Minerals Deep water cycling and partitioning must obey physical limits to the capacities of various water reservoirs in the planet. Although the surface water reservoir is essentially limitless,¹⁴ water has natural solubility limits in silicate minerals and melts. Mantle and crust minerals can store water in substantial quantities (e.g., Bolfan-Casanova 2005; Ohtani 2021; Mosenfelder et al. 2024) either as stoichiometrically hydrous minerals (e.g. serpentine, amphibole), or as non-stoichiometric -H or -OH in nominally anhydrous minerals or NAMs (e.g., olivine, orthopyroxene), the latter of which make up the bulk of silicate mantles. The ‘water-equivalent’ storage capacity in NAMs is related to the nature of the crystal lattice substitution enacted by -H or -OH, and depends on pressure, temperature, and redox conditions. Estimates of water content in the bulk present Earth vary widely, from one to an extreme 100 ocean masses (Peslier et al. 2017), but a recent estimate arrives at 2.6 to 8.3 ocean masses stored in the mantle and crust (generally below water saturation; Ohtani 2021). Of this total, only 0.3 to 0.4 ocean masses are in the crust (~0.21 in the continental crust), largely as stoichiometric hydrous minerals rather than NAMs, at concentrations of around 15,000–20,000 wt. ppm (Bodnar et al. 2013; Peslier et al. 2017).

In part because different NAMs are stable at different mantle depths according to temperature and pressure, and also because water concentrations at water saturation in NAMs are temperature-dependent, ‘water’ is not expected to be distributed homogeneously inside a planet. The typical assemblage of upper-mantle minerals will store about 10^2 to 10^3 wt. ppm water equivalent at water saturation (as compiled and re-fit by Dong et al. 2021). Meanwhile, in the 250-km-thick transition zone between the upper and lower mantles, the stable NAMs wadsleyite and ringwoodite can accommodate hydrogen equivalent to $1.8\text{--}2.3 \times 10^4$ wt. ppm and $1\text{--}1.25 \times 10^4$ wt. ppm water, respectively (Inoue et al. 2010; Tschauner et al. 2018). Wadsleyite/ringwoodite layers are predicted to be thermodynamically stable across many rocky exoplanets, implying that transition zone-like structures are common, with potential to hold much water, if filled — dominating the water storage capacities of planets up to ~1.5 Earth masses (Guimond et al. 2023). The water storage capacities of NAMs in lower mantle are debated, particularly that of bridgmanite, although the total seems to be much drier than the transition zone, at ~100–2000 wt. ppm water (e.g., Bolfan-Casanova et al. 2003; Karato 2015; Fu et al. 2019; Liu et al. 2021; Lu et al. 2025). Shah et al. (2021) and Guimond et al. (2023) estimated the water storage capability of rocky planets depending on mass and mineralogy, considering reasonable temperature and pressure variations with depth. Guimond et al. (2023) found that mineralogically-average rocky planet mantles would saturate at between about 2 and 8 Earth ocean masses, for planet masses from 0.5 to 5 Earth masses respectively, whereas Shah et al. (2021) find higher values due to using a much higher water capacity of postperovskite (3 wt.%), the high-pressure silicate dominating deep super-Earth mantles. Again, of course, mantles need not be saturated in water. Geophysical evidence reviewed in Ohtani (2021) suggests that Earth’s transition zone and upper mantle are quite far from water saturation (100–200 wt. ppm water in the upper mantle), and further, that the actual distribution of water in the transition zone itself is not homogeneous.

How do the water capacities of minerals affect how they move water into and through a planet’s deep interior? Hydrous minerals — chlorite, amphibole, serpentine — easily carry up to tens of wt.% water, but they tend to only be stable in cool regions of the interior, such as in the crust, and on a plate tectonics world, in subducted slabs of oceanic lithosphere.

¹⁴However, any steam atmosphere could not extend beyond a planet’s gravitational sphere of influence.

High-pressure hydrous phases (the ABC phases of Ringwood and Major 1967) can exist at deep lower mantle pressures of up to 60 GPa, on cool slab temperature-pressure profiles (not on typical mantle adiabats). These slabs where present — and mantle material viscously coupled to the slabs — can be major reservoirs of water, albeit transitory at geological time scales (e.g., Goes et al. 2017; Ohtani 2021; Keppler et al. 2024). In this way, subducted hydrous minerals play a key role in Earth's water ingassing mechanism. Possibly large yet difficult-to-estimate fractions of this subducted water are expelled at shallow depths, however (e.g., Höning et al. 2014). The remaining water, partly stored in serpentines and other hydrous minerals, then reaches the source depths of continental crust rock, where more hydrous minerals break down still, releasing water that is consumed to make new continental crust. In the end, a relatively small fraction of subducted water reaches the mantle itself. Some of the water will be released to the mantle wedge above the slab, where it may be incorporated into local NAMs; the descending slab may drag part of the hydrated mantle to even greater depth where water is eventually incorporated into lower mantle NAMs (e.g., perovskites, periclase, stishovite; Novella et al. 2024, Fig. 4). As a consequence, whereas the residence time of water in the very deep mantle may exceed 1 billion years, shallow dehydration operating on much shorter timescales could ultimately govern the upper-mantle water budget (Nakagawa 2023).

Differences in the water storage capacity between the mantle layers and phase transitions at the top and the base of the transition zone may have important consequences for the dynamics of Earth's mantle, such as initiating local melting where upwelling rock becomes supersaturated and dehydrates upon a mineral phase change (e.g., Bercovici and Karato 2003; Karato 2015; Ohtani 2021; Rüpke and Gaillard 2024, Fig. 4). The difficulty of redistributing water in the mantle through convection has been discussed by Richard et al. (2002) and Karato (2015). For example, the endothermic phase transition from ringwoodite to bridgmanite and magnesio-wüstite can cause a subducting slab to stall (e.g., Goes et al. 2017; Keppler et al. 2024) and inject water into the transition zone, rather than transporting it to the lower mantle.

Coupling Between Mantle Water, Dynamics, and Continental Crust Production Water can have a major effect on mantle flow by reducing the activation enthalpy for creep (e.g., Griggs and Blacic 1965; Hirth and Kohlstedt 2003; Karato and Jung 2003; Karato 2011). Further, the thermal conductivities of olivine (Chang et al. 2017), ringwoodite (Marzotto et al. 2020), and lower mantle mineral assemblages (Hsieh et al. 2020) have also been reported to decrease with increasing water content, and NAMs' water storage capacities themselves exhibit a strong temperature dependence (Karato 2015). The dependence of mantle flow on water content sets up potential feedback mechanisms (e.g., McGovern and Schubert 1989; Sandu et al. 2011; Höning et al. 2014; Höning and Spohn 2023). An increase in mantle water content will lower the viscosity so the mantle flows more vigorously. This enhanced flow will, in turn, increase the subduction rate (i.e. the ingassing rate) in a plate tectonics regime and amplify the initial increase in mantle water content. However, the faster mantle flow will also promote more water outgassing, dampening the positive feedback loop. This water-cycling process is coupled to the continental crust cycle through the contribution of wet, continent-derived sediments to water ingassing at subduction zones, and through the key role of water in the generation of granitic continental crust (Höning and Spohn 2023). The growth in land volume in these models compensates for the loss of surface ocean volume and tends to keep the average ocean depth constant. It is probably not surprising that these complex and intersecting feedback loops could produce bifurcations in both ocean volume and ocean basin capacity (topography); there may be more than one equilibrium solution for the same planetary conditions (compare Fig. 5).

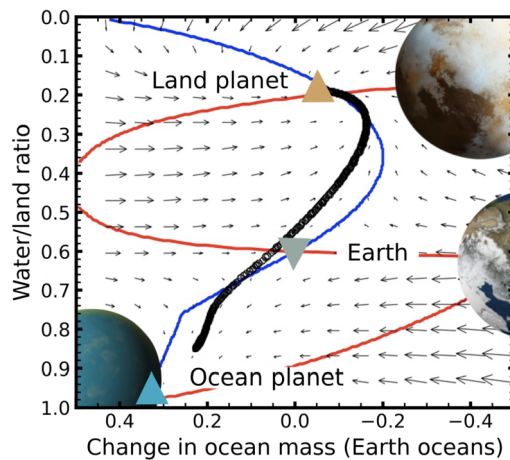


Fig. 5 Phase plane spanned by the surface ocean mass (expressed as the difference from one Earth ocean mass) and the coverage of the Earth's surface by continental crust, calculated by Höning and Spohn (2016) for present-day mantle temperatures. Local arrows are shown pointing in the direction of time evolution. Also shown are lines along which the rates of change of continental coverage (red) and ocean mass (blue) are zero. These lines intersect at three points (triangle markers) where both rates of change are zero, indicating equilibrium states. At the top fixed point (brown triangle; 'land planet'), the planet is at a stable equilibrium, mostly covered by continents; net ~ 0.1 ocean masses have been ingassed to the mantle. At the lower fixed point (blue triangle; 'ocean planet'), the planet is at another stable equilibrium, almost completely covered by oceans; net ~ 0.4 surface ocean masses have been gained from mantle degassing. The middle fixed point (grey triangle; 'Earth') is a saddle point, stable with respect to ocean mass but unstable with respect to continental coverage. The black circular markers indicate the endpoints of the 4.5 Ga evolution calculations, which do not necessarily reach equilibrium states. About 80% of the endpoints cluster around the 'land planet' fixed point; the lower fixed point is never reached because the mantle becomes too dry, cold, and viscous. Only a few percent of models end close to the 'Earth' saddle point. The models are initialised with randomly chosen temperatures between 1800 and 2100 K and with an inventory of one ocean mass in the mantle

What Controls Water Outgassing Rates? Rates of volcanic outgassing are an outcome of complex feedback loops involving both the surface and interior of the planet. Nonetheless, we can identify certain factors or conditions setting how efficiently a mantle outgasses water. The tectonic mode of the planet certainly appears crucial. Observing rates of volcanic melt production has not been possible for other rocky bodies outside the plate tectonics mode, excepting the heat-pipe archetype Io (where rates of crust production can be inferred from heat flux observations; O'Reilly and Davies 1981), so our estimates of volcanism rates in other tectonic modes come largely from inferences made on the basis of photogeological mapping and geodynamic modelling.

Across different models, stagnant-lid scenarios result in rates of volcanism diminished by approximately an order of magnitude compared to plate tectonics scenarios (Kite et al. 2009; O'Neill et al. 2013; Noack et al. 2016, 2017). Part of the difference in magma production rates can be explained by the ranges of depths where upwelling mantle will melt: under a very thick (~ 100 km), extremely viscous ('stagnant') global lid, upwelling stops at relatively high pressures, limiting adiabatic melting. Conversely, mantle convection essentially reaches the surface (at mid-ocean ridges) in the plate-tectonics mode. However, this explanation does not always extend to outgassing of water. Because water solubility in silicate melts increases quickly with pressure, water can remain largely dissolved in these melts at Earth's mid-ocean ridge pressures. Water outgassing from Earth's mantle is dominated instead by volcanic arcs, where melting is induced by adding water (Fig. 4).

Indeed, the pressure-dependence of water solubility may be an important accident of nature that controls water outgassing. In an influential study, Gaillard and Scaillet (2014) suggest that Venus' ~ 100 -bar atmosphere may prohibit the outgassing of any mantle water. Hence, through its modulation of the ocean depths overlying possible volcanic vents, the water/land ratio itself would also regulate water degassing. Water exsolution can be affected at ocean depths similar to terrestrial mid-ocean ridges, and has been predicted to virtually shut off for oceans deeper than 10 km (Krissansen-Totton et al. 2021).

As for overall rates of volcanism — the surficial expression of melt — some of the difference between tectonic modes is due to differences in the stress state of the lithosphere, among other factors. This discussion has not covered all of the factors that can affect water outgassing rates; an incomplete list follows. A 2D convection model of Archean Earth in the stagnant-lid mode (Guimond et al. 2021) found water outgassing rates correlating most strongly with the initial bulk mantle water content, the fraction of melt that extrudes as opposed to stalling deep in the crust, and mantle oxygen fugacity (increasing the gas phase $\text{H}_2\text{O}/\text{H}_2$). Nonetheless, for H_2 outgassing to be appreciable, melt oxygen fugacities must be lower by at least 4–6 orders of magnitude compared to modern Earth (Brachmann et al. 2025). Planet mass might be expected to influence outgassing at many stages of the process, through direct effects (higher gravity, interior temperatures, convective vigour) and indirect ones (likely tectonic modes). In 2D models, stagnant lid outgassing rates have been shown to increase with planet mass to a maximum at ~ 3 – 4 Earth masses, beyond which steep interior pressure gradients effectively shut off melting (Noack et al. 2017; Ortenzi et al. 2020); an appropriate treatment of melting in 1D can reproduce this behaviour (Kite et al. 2009). Melting the mantle requires heat, so planets with stronger internal heating — e.g., endowed with a greater concentration of radiogenic heat producing elements such as U, Th, and K compared with Earth — would experience more volcanism and outgassing, for longer (Frank et al. 2014; Nimmo et al. 2020; Unterborn et al. 2022), in a generally linear correlation best seen when low reference viscosities reduce the lag between internal heating and convective heat transport (Moore and Lenardic 2015; Unterborn et al. 2022). The greatest rates of volcanism in the solar system are observed on Io, which is tidally heated to the extent that its surface heat flow is $\sim 20\times$ Earth's despite its small size (e.g., O'Reilly and Davies 1981). Any convection-outgassing model will be sensitive to the assumed mantle solidus and the pressure at which melt becomes neutrally buoyant (Stolper et al. 1981), pointing to the important role of experiments in constraining these values in particular for non-Earth-like mantle compositions (Kiefer et al. 2015; Brugman et al. 2021).

In summary, for a water-bearing mantle to outgas water efficiently, two main characteristics are favoured: (i) a relatively thin lithosphere to promote adiabatic melting; and (ii) a relatively thin atmosphere and/or ocean to promote water exsolution from magma. The fact that so many other possibly relevant conditions are unconstrained means that quantitative predictions of water outgassing rates would be probabilistic. To expose the range of such predictions and give context to the rest of this article, Table 1 compares the water outgassing rates from a selection of mantle convection models. Interestingly, stagnant-lid convection models produce a similar maximum water outgassing rate of 0.2–0.3 ocean masses per Gyr across different model setups and assumptions. Plate tectonics models consistently produce a larger maximum water outgassing rate of 1–10 ocean masses per Gyr. Plate tectonics models tend to use more diverse parameterisations; notably, where outgassing depends solely on mantle temperature in Schaefer and Sasselov (2015) and Komacek and Abbot (2016), outgassing rates drop to order ~ 0.01 – 0.1 ocean masses per Gyr. We offer the provisional conclusion that long-term water outgassing rates far exceeding 10 ocean masses per Gyr would require unusual conditions that are not normally considered in rocky planet thermal history models.

Table 1 Selected volcanic H₂O outgassing fluxes for a ~1 Earth mass planet from mantle thermal history models. Variations in tabulated outgassing fluxes are not only due to differences across the columns listed here; see the original publications for details. Note earlier publications of a similar model are omitted (as are those which do not clearly provide an H₂O outgassing flux). The numbers in the square brackets, separated by commas, represent ranges of the assumed parameters and results. f_{O_2} is the mantle oxygen fugacity expressed as the log difference from modern Earth. OM: Ocean Masses (1 OM = 1.34×10^{21} kg); PCT: 0/1D parameterised convection theory; MLT: 1D mixing length theory; PT: plate tectonics; SL: stagnant lid; UM: upper mantle

Reference	Model	Mantle water (wt. ppm)	f_{O_2} (ΔE_{Earth})	Mode	Flux (OM Gyr ⁻¹)
Sandu et al. (2011)	PCT	[689, 2068]	0	PT	[0.01, 8]
Komacek and Abbot (2016)	PCT	[470, 720]	0	PT	[0.01, 5]
Krissansen-Totton and Fortney (2022)	PCT	[30, 30,000]	[-4, 3]	PT	[~0, 16]
Höning and Spohn (2023)	PCT	~80 (UM)	0	PT	[0.03, 0.07]
Tosi et al. (2017)	PCT	[250, 1000]	0	SL	[0.003, 0.03]
Miyazaki and Korenaga (2022a)	PCT	[100, 1000]	0	SL	[0.007, 0.2]
Spaargaren et al. (2020)	MLT	695	0	SL	0.7
Spaargaren et al. (2020)	MLT	695	0	PT	<4
Guimond et al. (2021)	2D	[50, 450]	[-6, 0]	SL	[0.004, 0.3]
Nakagawa (2023)	2D	<10,000	0	PT	[0.008, 8]

3 Consequences of Water Versus Land Surfaces on Climate and Life

The whole spectrum of water/land ratios is possible on rocky worlds: by now we hope to have moved beyond viewing modern Earth as default. This notion matters because planets' land and water masses perform several important functions in controlling and regulating both surface temperature (and hence the planet's location with respect to the classic circumstellar habitable zone) and biological productivity. The importance of land versus ocean surfaces is also, notably forefronted in origins of life scenarios (e.g., Deamer et al. 2022). For example, Darwin's hypothesis that life begins in 'warm little ponds' — such as hot springs on subaerial volcanic platforms — is finding increasing support in geological evidence (e.g., Djokic et al. 2017; Van Kranendonk et al. 2021), prebiotic chemical modelling (e.g., Pearce et al. 2017), and laboratory experiments (e.g., Mulikidjanian et al. 2012; DeGuzman et al. 2014). The major competing idea, origin of life at hydrothermal vents on the seafloor, meanwhile requires the existence of oceans and a geologically active seafloor (Corliss et al. 1981). Whether early Earth's actual subaerial land fraction was minute (Chowdhury et al. 2025) or substantial (Armstrong 1981; Rosas and Korenaga 2018) then becomes highly relevant to either scenario's favourability. Heated debate continues as to the environment in which life began on this planet: warm little ponds, hydrothermal vents, or somewhere else (e.g., Baross and Hoffman 1985; Bada 2004; Damer and Deamer 2020; Russell 2021; Westall et al. 2023a; Walton et al. 2024). Although planet Earth is just one case study, recent works reviewed in this section have employed theoretical models to test how these consequences of the water/land trade-off might play out across exoplanetary parameter space.

3.1 Consequences for Planetary Climate

A planet's water/land ratio affects its climate through two primary mechanisms: (i) changing planetary energy balance via surface albedo (see Sect. 3.1.1 below); and (ii) the role of

water and erosion in the carbonate-silicate thermostat (Sect. 3.1.2). Secondly, climate is also affected by the geographic distribution of land (e.g., supercontinents, equatorial versus high-latitude land) and by topographic relief (e.g., Glaser et al. 2025; Salazar et al. 2020; Macdonald et al. 2022; Del Genio et al. 2019b; Way et al. 2021).

3.1.1 Surface Albedo Effects

Albedo — the ratio of reflected to incident light — is a main factor in the energy balance of a planet. All else being equal, planets with high-albedo surfaces are cooler because they reflect more incident radiation to space. For example, although ice and snow reflect $\sim 80\text{--}90\%$ of incoming radiation from a G-dwarf star, liquid water reflects only $\sim 5\%$, absorbing the rest. Albedo is wavelength dependent, therefore both the surface composition as well as the incident stellar spectrum are important. Radiation from M-dwarf stars peaks in the near-infrared; under such a stellar spectrum ice and snow have 35–70% lower albedo and absorb more incoming radiation compared with G-dwarf stars (the albedo decrease under K-dwarf stars is 6–17%; Pierrehumbert 2011; Shields et al. 2013). Ice and snow, however, are always more reflective than an ocean, leading to an ice-albedo feedback effect (see next paragraph; Shields et al. 2013). Given relatively small land/water ratios (e.g., on Earth), ocean-absorbed heat has a major effect on climate; heat is redistributed via ocean circulation to maintain relatively moderate ocean surface temperatures across diurnal and seasonal cycles (Rahmstorf 2002). Meanwhile, land reflects more energy compared with oceans — lowering the total energy in the system — and moreover cannot efficiently redistribute this energy spatially, leading to large diurnal and seasonal variations in temperature on continents. In this way, the evolution of continents (see Sect. 2.1.2) has affected Earth's global energy balance.

Aside from vegetation cover, land surface albedo is largely affected by mineralogy. A clear distinction can be drawn between more primitive, ubiquitous basaltic crusts rich in dark mafic minerals (albedo ~ 0.1), and the light-coloured felsic crust typical of Earth's processed continents (albedo ~ 0.35). Indeed, Earth's bare felsic mineral surfaces are among the brightest found on the terrestrial planets in the Solar System (see Lustig-Yaeger et al. 2026, this topical collection for a discussion of exoplanet crust mineralogy and its albedo signatures).

Perhaps the most notorious surface albedo- and climate-related phenomena is the ice-albedo feedback. Upon freezing, the albedo of water increases drastically, from ~ 0.05 to ~ 0.9 . A decrease in temperature creates more ice, reflecting more radiation to space, further cooling temperatures — and giving rise to a positive feedback loop (Thackeray and Hall 2019; Zhang et al. 2022). The ice-albedo feedback is best exemplified by the 'snowball Earth' glaciations of the Neoproterozoic (e.g., Fairchild and Kennedy 2007; Chandler and Sohl 2000; Spiegel et al. 2010, among others). These glaciation periods were likely triggered, at least in part, by changes in orbital parameters (the Milankovitch cycle); the positive nature of the ice-albedo feedback led to a runaway snowball climate (Spiegel et al. 2010). Further, the presence of land has a large effect on the stability and lifetime of ice, as seen by comparing Earth's Arctic to Antarctic poles. Because oceans are able to circulate heat from warmer latitudes, polar sea ice may melt during the summer. Continual, multi-year sea ice in the Arctic is restricted to latitudes north of $\sim 80^\circ\text{N}$ in the pre-industrial climate (Walsh et al. 2017; Comiso 2023), whereas ice sheets have persisted on the Antarctic continent for millions of years (Yamane et al. 2015). The generally-decreasing albedo of ice with increasing wavelength (and hence peak radiation from increasingly smaller stars) means that the ice-albedo feedback is expected to be muted on planets orbiting M-dwarfs, and may even reverse into a stabilising feedback at high water/land ratios (e.g., Shields et al. 2013; Rushby et al. 2019).

3.1.2 Continents and the Carbonate-Silicate Weathering Thermostat

Earth's clement climate is maintained over geological timescales by the carbonate-silicate cycle (Walker et al. 1981; Gislason et al. 2008; Pogge Von Strandmann et al. 2021; Arnshardt and Rothman 2022; Brantley et al. 2023). The negative nature of this feedback maintains a climate equilibrium, where global mean temperatures have remained at $\sim 10\text{--}35^\circ\text{C}$ for the last 450 Ma (Judd et al. 2024). The carbonate-silicate cycle balances greenhouse CO_2 concentrations via the temperature-dependent removal of CO_2 via reactions with calcium carbonate (CaCO_3). When CO_2 concentrations are high and the climate is warm, precipitation is stronger (increased water vapour capacity in the atmosphere) and more acidic (CO_2 dissolves into water to form carbonic acid). The acidic rain erodes and chemically weathers silicate rocks, releasing ions including calcium. Weathered calcium reacts with aqueous CO_2 (in the form of HCO_3^-) to produce calcium carbonate precipitate. This net process removes CO_2 from the atmosphere, reducing the temperature. Presumed constant over the timescales of this weathering process (hundreds of thousands of years) is the volcanic release of CO_2 through outgassing. Therefore, when temperatures are cooler, less CO_2 is removed from the atmosphere, but the same amount is introduced, increasing the atmospheric concentration and hence the surface temperature. Although the quantitative details of Earth's carbonate-silicate weathering thermostat are not settled, some form of negative climate feedback seems far more likely than a chance balancing of surface carbon sources and sinks (Coogan and Caves Rügenstein 2025).

The carbonate-silicate cycle, as we understand it, may require both exposed land and water to work effectively from both sides (Lingam and Loeb 2019; Glaser et al. 2020; Krissansen-Totton et al. 2021):

1. As argued by, e.g., Glaser et al. (2020), seafloor weathering is less effective than subaerial continental weathering. The reasons are twofold: (i) decreased physical erosion (rivers have much higher velocity than seafloor currents) and (ii) increased pH in the ocean (Earth's ocean pH ~ 8.2). Physical erosion serves to increase the surface area of the substrate, increasing weathering, and low, acidic pH serves to increase chemical weathering rates. For extremely deep oceans — hundreds of kilometres — high-pressure ice (Léger et al. 2004; Noack et al. 2016) would seem to decouple any eroded rocky material from dissolved oceanic carbon, breaking the loop.
2. Volcanism and outgassing may be suppressed on planets with deep global oceans. CO_2 would be more soluble in (i.e., exsolve less from) magma under higher pressures, so CO_2 outgassing may be orders of magnitude lower than if it were degassing subaerially (Krissansen-Totton et al. 2021). Further, silicate melt itself could be denser than the ambient mantle at these high overburden pressures (i.e., with oceans $\gtrsim 400$ km deep), and so would not rise via buoyancy forces to the surface (Stolper et al. 1981; Noack et al. 2016). Inefficient CO_2 outgassing may lead to a runaway snowball state.

Nevertheless, the kinetics of seafloor weathering remain ambiguous; several studies have argued that seafloor weathering could still be an efficient carbon sink under high-enough geothermal heat flux (e.g., Coogan and Gillis 2013, 2018; Coogan and Dosso 2015; Krissansen-Totton et al. 2018; Nakayama et al. 2019). More recent studies have begun to consider how effectively atmospheric CO_2 -regulating processes might work under various extraterrestrial conditions, including crust mineralogy (Hakim et al. 2021) and high CO_2 itself (Graham and Pierrehumbert 2024).

3.1.3 Planetary and Numerical Experiments

In the record of Earth's supercontinent cycle, we might extricate a kind of planetary test of the relationship between changing land area and distribution on one hand, and atmospheric CO₂ and temperatures on the other hand. The assembly of Pangaea is associated with a marked decrease in global sea level (hundreds of metres), a decrease in CO₂ partial pressure (a few thousand ppm), and an ensuing icehouse climate; vice versa for Pangaea's breakup (Nance 2022, and references therein). Falling sea levels have been explained by supercontinents' thermal uplift and more voluminous ocean basins across the planet (Worsley et al. 1984). Atmospheric CO₂ changes follow from changes in continental weathering: not only does the falling sea level expose more land, but the colossal act of assembly means more erosion and chemical weathering, drawing down CO₂. Some studies have attempted to close the loop by pointing out ways global climate could itself affect mantle circulation, implying complex geological couplings through the whole planet (Foley and Driscoll 2016; Jellinek et al. 2020).

Absent any other geological record, an important tool for testing how water/land ratios and configurations influence planetary climate is a general circulation model (GCM). GCMs become especially useful for exploring the exotic climates of exoplanets with wholly non Earth-like orbital parameters such as 1:1 spin-orbit resonance (i.e., tidally locked). The climate of tidally locked planets are of interest as most habitable zone exoplanets in M-dwarf systems are likely tidally locked (Barnes 2017). Pioneering 3D GCM studies have demonstrated possible 'eyeball' climate states on these tidally locked, habitable zone exoplanets, where liquid water would be stable directly under the star (the substellar point), given surface oceans at least ~10% the mass of modern Earth's (e.g., Pierrehumbert 2011; Yang et al. 2014; Turbet et al. 2016). Drier planets may see a longitudinal ring of temperate conditions, along the permanent 'evening' terminator, due to reduced heat transport in the atmosphere (Lobo et al. 2023). If realistic ocean heat transport (i.e., dynamic ocean) is included in the GCM, then the 'eyeball' appears to stretch into a 'lobster' (e.g., Hu and Yang 2014; Yang et al. 2014; Del Genio et al. 2019a). Later works have begun introducing new continent configurations to the experiment (e.g., Lewis et al. 2018; Salazar et al. 2020; Zhao et al. 2021; Macdonald et al. 2022; Way 2025) — in particular, featuring variations on the theorised scenario of such planets having single large landmasses/basins continuously re-oriented to the substellar point, via true polar wander (Leconte 2018), like the Moon (Zuber et al. 1994). These experiments have concluded that increasing (dayside) water/land ratio decreases global mean temperature by ~20 K, mostly via increasing the planetary albedo, although the substellar point locally heats up. In fact, the dayside may become a desert, reducing the evaporation of water vapour from the ocean into the atmosphere (and thus the impact of this water vapour on longwave radiation). Similar trends have also been shown in simpler energy-balance models (Rushby et al. 2019; Höning and Spohn 2023). These consequences of land/water surface albedo on global mean temperature persist across different stellar spectral classes, from M- to F- dwarfs, despite the changes to absolute albedos of land and water (Rushby et al. 2019). However, in F-G-K systems, continental configurations may be less important, since habitable zone exoplanets in these systems are likely not tidally locked (i.e., fast rotating) and do not have permanent day/night sides (Glaser et al. 2025). Overall, the complexities of atmosphere and ocean heat transport, and the sensitivity of surface albedo to host star spectrum, mean that when investigating a specific planet in practice, a number of targeted simulations should be carried out to delineate a range of possible climates.

3.2 Consequences for Life

The biomass on modern Earth is not evenly distributed between land and oceans (Bar-On et al. 2018). While terrestrial biomass comprises 470 Gt carbon of mostly plant life (autotrophic, although only one third is active), marine biomass totals 6 Gt carbon of mostly heterotrophic life. Motivated in part by this simple observation, we can ask how and why the planetary land fraction would affect a propensity for biological productivity. Tightly linked with both land fraction and life is climate: productivity in the seas depends on sea surface temperature, for example; and such effects have been studied through coupling climate and biogeochemical models (Lerner et al. 2025). Here we focus on direct trade-offs of water versus land surfaces on life.

3.2.1 Net Primary Productivity

Comparing markers of biological productivity between Earth's land and oceans provides a clue to the hypothetical consequences of water/land ratios on life. Net primary productivity (NPP) encapsulates the net amount of organic carbon produced through photosynthesis (expressed in units of kg C yr^{-1}). It regulates many facets of the biosphere (Schlesinger and Bernhardt 2013). In the case of Earth, the terrestrial and marine NPP are roughly equal to each other (Field et al. 1998; Ito 2011). The lesser areal proportion of land means that NPP per unit area is greater on land than in the oceans. As mentioned above, the modern land biomass ultimately dominates the marine biomass by about two orders of magnitude (Bar-On et al. 2018) — though Sect. 3.2.2 will note how this fact does not hold for all of Earth history. The large difference in biomass and smaller difference in NPP seem related to how biomass is distributed across trophic levels: marine life is overabundant in consumers, which build biomass inefficiently compared to primary (photosynthesising) producers; moreover, land-based producers tends to have a longer turnover time (Hatton et al. 2015; Bar-On et al. 2018). If the physical mechanisms behind marine life's inverted food pyramid (see Burgess and Gaines 2018) would operate elsewhere, then other marine biospheres may be similarly less productive than their land equivalents.

On Earth, the maximum NPP across more than half of all land area is limited by access to liquid water resources (Churkina and Running 1998). On land planets with limited water inventories, it is conceivable that the surface hydrological cycle would serve as a bottleneck on NPP, albeit not the only such control (e.g., temperature is another key determinant). Meanwhile, Earth's marine biosphere is limited by nutrient availability: chiefly phosphorus (P) in the form of phosphates, delivered by way of continental weathering (Schlesinger and Bernhardt 2013). Whilst there has been debate about what nutrients serve as the ultimate bottleneck on NPP, many works support phosphorus in not just the Phanerozoic, but also the Archean and the Proterozoic eons (Tyrrell 1999; Laakso and Schrag 2018; Hao et al. 2020; Zhao et al. 2024). Several works have suggested that NPP on ocean worlds could be stymied by dissolved P availability because of diminished continental weathering (Lingam and Loeb 2019, 2021; Glaser et al. 2020; Olson et al. 2020). A simple model developed by Lingam and Loeb (2019) in this context suggested that the NPP and biomass of both (water-limited) land and (nutrient-limited) ocean planets are potentially orders of magnitude lower than on Earth.

However, alternative pathways for nutrient supply to marine biospheres may be found in oceanic crust weathering and/or serpentinisation (Syverson et al. 2021; Pasek et al. 2022). Besides phosphorus, other candidates for the limiting nutrient are nitrogen (as nitrates; Tyrrell 1999; Bristow et al. 2017), iron (Bristow et al. 2017; Wade et al. 2021), or trace

metals such as molybdenum (Anbar and Knoll 2002). The factors potentially modulating the availability of these alternative limiting nutrients on a given planet range from volcanic outgassing rates and hydrothermal activity to atmospheric redox states (e.g., Lingam and Loeb 2019). In any case, we highlight that the same single ingredient need not limit biological productivity for the entire history of life on a planet. Wade et al. (2021) propose that it was the *decrease* in environmental Fe^{3+} availability after the Great Oxygenation Event that eventually led to the evolution of multicellular life, able to efficiently recycle iron within one organism.

This discussion has painted a heuristic picture of how NPP could be sensitive to a planet's water/land ratio, but many other aspects are potentially important. For instance, provided that nutrient availability is not a constraint, the average ocean depth plays a key role in governing NPP. Most biological productivity in Earth's oceans occurs in the top ~200 m (Sigman and Hain 2012), stemming from a combination of nutrient mixing and upwelling driven by wind and tidal forces (Rykaczewski and Checkley 2008), as well as sufficient photon fluxes for photosynthesis (Sarmiento and Gruber 2006). On planets that experience strong tidal forces — either from the host star or a large moon — it is conceivable that enhanced tidal mixing might help boost NPP (Lingam and Loeb 2018; Olson et al. 2020), if all other factors are held fixed.

Atmospheric Oxygen On Earth, the NPP also shares close links with the production of molecular oxygen (O_2) because the predominant pathway for biosynthesis is oxygenic photosynthesis. As a result, worlds with low NPP would be expected to have limited fluxes of O_2 production. Hence the endmember water/land ratios of 0 or 1 may be associated with low atmospheric O_2 levels even on inhabited planets; this qualitative reasoning is broadly supported by simple quantitative models (Lingam and Loeb 2019, 2021; Watanabe and Tajika 2021). We add the caveat that atmospheric O_2 levels are governed not only by O_2 sources (oxygenic photosynthesis) but also by sinks, determined by weakly bound variables such as carbon burial efficiency and the flux of reducing gases.

If the prediction that all-land or all-ocean planets have lower atmospheric O_2 is valid, further evolutionary consequences become apparent. It has been proposed that a relatively high concentration of atmospheric oxygen is a prerequisite for the emergence and/or diversification of complex multicellularity, given the bioenergetic advantages of aerobic respiration (Knoll 1985; Catling et al. 2005). Likewise, O_2 levels comparable to modern Earth might be valuable or even necessary for technological intelligence (Lingam et al. 2023; Balbi and Frank 2024; Stern and Gerya 2024).

3.2.2 Life in Deep Time

The origin and diversification of life on Earth both seem to be inseparable from its patterns of land and ocean coverage. For each mechanism to which we may owe the beginnings of life on early Earth, the water/land ratio seems to matter (e.g., Scherf et al. 2024, and references therein). Ocean planets are unable to facilitate the wet/dry cycles critical to the warm little ponds origin of life hypothesis; land planets lack the redox and elemental gradients key to the alkaline submarine hydrothermal vent origin of life hypothesis. Either way, there will not be a clear sense of change of biological diversity with increasing water/land ratio, if only for the fact that evolution has a nonlinear history. The fossil record suggests that the biosphere occupied land only from the Phanerozoic onwards (e.g., Awramik and McNamara 2007): land life owes itself to earlier evolution in the oceans.

Planetary land fractions and their evolution in time (e.g., supercontinent cycles) would then go on to influence how (complex) life might evolve. By drawing on the major evolutionary transitions that unfolded on Earth (Szathmáry and Maynard Smith 1995) — some of which definitely occurred on land, with others unfolding in water — Lingam and Loeb (2019) suggested that the relative odds of these events occurring on either pure-land or pure-ocean worlds is suppressed by orders of magnitude relative to Earth. The optimal chances for major evolutionary transitions to complex life could be found on worlds with roughly equal surface fractions of landmasses and oceans.

In their discussion of so-called ‘superhabitable’ worlds, Heller and Armstrong (2014) raised the point that it was not just the total area of landmasses or oceans that would be crucial, but also their distribution. Indeed, empirical trends documented on Earth show that coastal benthic environments are more diverse than open water (Gray 1997). This theme was elaborated by Lingam and Loeb (2021, Chap. 5.6) by drawing on established models from theoretical ecology (Rosenzweig 1995; May and McLean 2007; Harte 2011), chiefly the principle of maximum entropy and the species-area relationship, to outline how land distributed over smaller regions could conceivably yield greater biodiversity than a single supercontinent having the same area.

Moreover, biodiversity is observed to correlate with tropical regions that may change with time due to continental drift. As Alexander von Humboldt (1769–1859) already knew, mountain belts, particularly the Andes, are exceedingly rich in biodiversity (Rahbek et al. 2019). In a similar vein, marine animal diversity has been observed to increase during the breakup of supercontinents (Zaffos et al. 2017), possibly stemming from changes in the areas of continental, coastal, and deep water environments. The converse might arise during the assembly phase. This apparent correlation between speciation and the supercontinent cycle raises the possibility that worlds upon which this cycle operates on different timescales — or essentially not at all (e.g., on ocean worlds) — might display speciation dynamics distinct from Earth.

4 Observing Water/Land Ratios and Evaluating the Presence of Life

Seeing oceans, continents, quasi-static weather patterns, atmospheric and surface biosignatures, and even artificial structures on exoplanets would all be clues for detecting and characterising life outside the Solar System. In fact, as discussed in the previous sections, the water/land ratio itself can inform us about a planet’s climate and possible geodynamics, as well as the feasibility of extant life-as-we-know-it and its diversity.

This section first reviews recent modelling efforts to extract planetary surface coverage information from (hypothetical) observations of rocky exoplanets and their validation from Earth observations. Then, it elaborates on future astronomical observational capabilities to collect necessary data and obtain the first maps of rocky exoplanets in habitable zones.

4.1 Mapping Surfaces of Temperate Rocky Exoplanets and Evaluating Their Water/Land Ratio

Time-series measurements of the light reflected from an exoplanet, recorded over the course of the planet’s axial rotation and orbital motion — that is, light-curves — contain information on structures on the planetary surface, as well as in the atmosphere and near-planetary space. Such one-dimensional (1D) time-series of light-curves can provide two-dimensional (2D) time-averaged albedo maps with structures resolved in both longitude and latitude. For

more than hundred years, a deconvolution of the longitudinal and latitudinal information has been proven to be feasible, thanks to a favourable combination of the axial planet rotation — revealing different hemispheres — and different illumination and reflection angles due to planet orbital motion, especially when the axial and orbital inclination (obliquity) directions are misaligned.

Model solutions obtaining albedo maps, along with the spin-orbital parameters, from reflected flux or polarization light-curves have been previously demonstrated for angularly unresolved planets, moons and asteroids in the Solar System, for and various types of exoplanets, from hot Jupiters to Earth-like (e.g., Russell 1906; Guthnick 1906; Morrison et al. 1975; Buie et al. 1997; Kaasalainen et al. 1992; Carbognani et al. 2012; Cowan et al. 2009, 2017; Fluri and Berdyugina 2010; Fujii et al. 2010; Kawahara and Fujii 2011; Fujii and Kawahara 2012; Schwartz et al. 2016; Lustig-Yaeger et al. 2018; Farr et al. 2018; Berdyugina and Kuhn 2019; Fan et al. 2019; Aizawa et al. 2020; Kawahara 2020; Kawahara and Masuda 2020; Asensio Ramos and Pallé 2021; Gu et al. 2021, 2022; Kuwata et al. 2022; Teinturier et al. 2022). These works differ by assumptions and by numerical approaches to forward modelling and deconvolution (inversion) of light-curves, which affect properties of inferred ‘best’ solutions and their uncertainties; that is, how one starts from simple 1D back-projection ‘maps’ to 2D principle-component maps and pixel-wise inversions that result in multi-colour 2D maps. Assumptions have differed about, for example, star-planet geometries and compositions of the planetary surface and atmosphere. Methods for mapping surfaces of exoplanets (exo-cartography) have been previously reviewed by Berdyugina et al. (2019) and Cowan and Fujii (2020).

In the context of future capabilities for reflected light detections from rocky exoplanets, many of the above-cited works have validated the principles of exo-cartography using Earth as an available test-case of such exoplanets. Since Sagan et al.’s analysis of Earth observations by the Galileo spacecraft (Sagan et al. 1993), Earth-as-an-exoplanet data have been obtained from the EPOXI mission (e.g., Cowan et al. 2009, 2011; Robinson et al. 2011; Fujii et al. 2011), the NASA Earth Observatory (NEO; e.g., Berdyugina and Kuhn 2019), the Moderate resolution Imaging Spectroradiometer (MODIS; e.g., Kawahara and Fujii 2011; Mettler et al. 2020; Kelkar et al. 2025), the Deep Space Climate Observatory (DSCOVR; e.g., Jiang et al. 2018; Fan et al. 2019; Aizawa et al. 2020; Gu et al. 2021, 2022; Kuwata et al. 2022), and the Lunar Crater Observing and Sensing Satellite (LCROSS; e.g., Robinson et al. 2014).

Since dry land is typically of a higher average albedo compared with the very low albedo of water oceans (Sect. 3.1.1), and since (Earth-like) land vegetation has characteristic spectral and polarised reflectance (Sagan et al. 1993; Seager et al. 2005; Kiang et al. 2007a,b; Berdyugina et al. 2016; Arp et al. 2020), inversions that are robust to measurement errors can reveal contours of continents, even for sparsely-measured and noisy light-curves (Fig. 6). Thus the water/land ratio is the first, immediate outcome of reflected light-curve inversions, if land masses and oceans are both present, and if the entire planetary surface is observed and visible at a given wavelength. For exoplanets that are tidally-locked at different spin-orbital resonances (e.g., Proxima b), extracting a water/land ratio on an observable part of the planetary surface was demonstrated by Berdyugina and Kuhn (2019): the continents can be well mapped if present in the star-facing planetary hemisphere.

A common issue remaining in all map inversion techniques lies in how to account for time-variable clouds (weather) and surface features (seasons). For example, using MODIS data, Kawahara and Fujii (2011) showed that light-curve inversions can recover an approximate cloud distribution, whereas inversion of light-curve *differences* between near-infrared

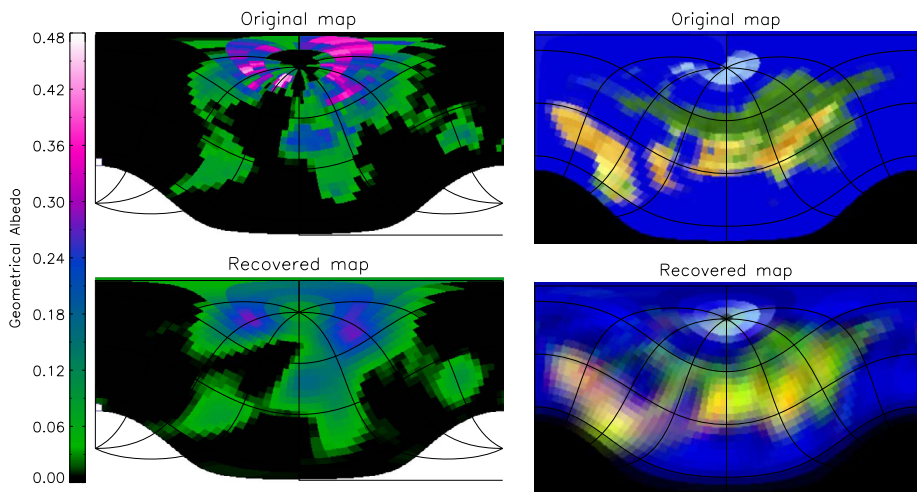


Fig. 6 Model cases for a distant Earth-like exoplanet indirectly imaged using the ExoPlanet Surface Imaging technique (EPSI; Berdyugina and Kuhn 2019). *Left:* The original map is based on NASA Earth Observatory albedo data from March 2003. The recovered map is obtained by inversion of a reflected light curve synthesized using the original map, assuming a signal-to-noise ratio of 200 and a total number of measurements of 3000. *Right:* The original map is based on a composite (RGB) Earth image (similar to that in Fig. 1) with parts of the terrestrial continents arranged in a plausible pattern. The recovered map is inferred from four broad-band (optical to NIR) reflected light curves. Continents and their spectral features are well recovered (for details, see Berdyugina and Kuhn 2019)

(0.8–0.9 μm) and blue (0.4–0.5 μm) bands roughly recovers the water/land distribution, except for at high-latitude regions persistently covered with clouds and snow. This study considered the case of a partially cloudy mock Earth-twin on a face-on orbit. From time-series of NEO albedo data, Berdyugina and Kuhn (2019) inferred realistic surface albedo maps with varying cloud cover, as well as time-dependent partial maps showing seasonal changes in surface vegetation and ice cover. In other works (Fan et al. 2019; Aizawa et al. 2020; Kuwata et al. 2022), two principle components ascribed to land coverage and to ‘surface-independent’ cloud coverage were extracted from DSCOVR data; Earth’s 2D water/land distribution was roughly reproduced. Teinturier et al. (2022) tested a cloud-removal scheme using DSCOVR observations, but found it difficult due to the necessarily full-phase data. Motivated by the need to account for cloud and surface variability, further advancement in numerical approaches, such as Bayesian dynamic mapping (Kawahara and Masuda 2020) and regularization learned from mock surfaces (Asensio Ramos and Pallé 2021), has delivered model reconstructions of large-scale evolving patterns. Interpretation of such high and low albedo patterns on real exoplanets with unknown geography and weather varieties will nonetheless be a challenge.

How much detail can be inverted from an exoplanet’s reflected light? For sufficiently high signal-to-noise ratio ($S/N \sim 20$ or more) and number of measurements (200 or more), the ExoPlanet Surface Imaging (EPSI) technique of Berdyugina and Kuhn (2019) could detect surface features down to about 2% of the total exoplanetary surface area, such as Sahara desert (1.8%) and Australia (1.5%; see Fig. 6). Aizawa et al. (2020) also showed that low-noise and frequent measurements of exoplanets comparable with the disk-integrated DSCOVR Earth data are needed to produce reliable results. Kawahara and Fujii (2011),

employing simulated Earth-twin data also with $S/N = 20$, were able to infer large-scale cloud cover and surface structures.

Even more detail would be possible with multi-wavelength light-curve measurements (optical to near-infrared bands). These observations could provide ‘photographic’ views of distant exoplanets, analogous to Earth images (Fig. 1) but certainly at a lower spatial resolution. In Berdyugina and Kuhn (2019), this ability was demonstrated for Earth, other Solar System planets and moons, and simulated exoplanets with Earth-like life and various artificial structures. In particular, low-resolution reflected spectra consisting of only four broad-band measurements sufficed to distinguish spatially resolved patches of various surface compositions, such sand and vegetation. Similarly, Kawahara (2020) demonstrated performing a spectral retrieval (ten photometric bands) of several surface components for a composite colour surface map of Earth as an exoplanet. Hence such multi-wavelength images of exoplanets would in principle provide information on the surface composition, geology, geodynamics, climate, and possibly even the presence of life.

The geographic location of land masses with respect to the equator and poles can be also well documented in such maps (Fig. 6). This result is achieved via a simultaneous retrieval of the map and spatial orientation of the spin and orbital axes of the planet in several currently employed methods. In particular, the obliquity of the spin axis with respect to the orbit may inform us about planet’s possible seasons and climate zones, similar to those on Earth. Errors on the spin-orbital parameters can vary depending on the quality of data. However, an additional constraint on planetary obliquity with respect to the observer would be provided by the detection of a polar ice cap (Berdyugina and Kuhn 2019).

A completely different approach to mapping exoplanetary surfaces is based on the remarkable optical properties of the solar gravitational lens (SGL), whose focal line begins at ~ 540 AU from the Sun. The SGL can be employed to focus light from a faint, distant source along that line by bending photon trajectories. Advantages include major brightness amplification by a factor of $\sim 10^{11}$ at the wavelength of $1 \mu\text{m}$ and extreme angular resolution of $\sim 10^{-10}$ arcsec within a narrow field of view (Turyshchev and Toth 2017). To make use of this opportunity, it was proposed to position a telescope beyond ~ 540 AU and use the SGL to magnify light from distant objects on the opposite side of the Sun; for example, from Proxima b (Eshleman 1979; Maccone 2009; Turyshchev and Toth 2017; Turyshchev 2018; Turyshchev and Toth 2022). Technical feasibility studies for such an interstellar space telescope are being carried out (e.g., Turyshchev and Toth 2023). The SGL telescope may deliver unprecedented high-resolution imaging and spectroscopy of terrestrial exoplanets within $\sim 30\text{--}100$ parsec from the Sun, as a possible follow-up mission for the most interesting target.

4.2 Future Facilities for Mapping Surfaces of Potentially Habitable Exoplanets

Detecting reflected light from rocky exoplanets in habitable zones of cool main-sequence stars — i.e., G-, K- and M-type dwarfs — is currently beyond capabilities of optical astronomical facilities on the ground and in space. The observations are difficult because the reflected light from the planet is many orders of the magnitude dimmer than the direct light from the star. A detection of these planets’ reflected light at high S/N requires an imaging contrast of at least 10^{-8} to 10^{-10} , for planets around early M-dwarfs to early G-dwarfs, respectively. Achieving such a high imaging contrast requires special optical designs and data calibration techniques: stellar coronagraphy and high angular resolution, for example. Also required to reduce the stellar light contamination in the reflected light is a large angular separation between the host star and its planet.

These optical requirements can be in principle achieved with extremely large-aperture ground-based telescopes, such as the Extremely Large Telescope (ELT); the Giant Magellan

Telescope (GMT), or the Thirty Metre Telescope (TMT). Considering the imaging contrast achieved so far with existing large ground-based telescopes (e.g., the Very Large Telescope, VLT; Gemini), which is about 10^{-6} to 10^{-7} , the coming generation of extremely large telescopes may be suitable for indirect light-curve imaging of rocky exoplanets in the habitable zones of late (coolest) M-dwarfs and early (hottest) brown dwarfs, if these observatories achieve a similar contrast (e.g., for ELT, current efforts are focused in the infrared, Feldt et al. 2024). For instance, observations of Proxima b with a 30–40 m aperture telescope may deliver reflected light measurements with S/N of 10 to 100 in the photometric BVRI-bands (i.e., blue-to-infrared), respectively, for an exposure time of only one hour, when assuming reasonable planetary parameters and telescope efficiency (Berdyugina and Kuhn 2019). A 20 m-class telescope may be able to achieve an S/N of 5–20 in the BVRI-bands in one hour. In fact, several dozens of habitable zone exoplanets around M-K-G-dwarfs within the solar neighbourhood (limited by the stellar magnitude; brighter than $V = 13$ mag) can be detected in reflected light with $S/N \geq 5$, using a 25-m telescope within eight hours of total exposure time. Several high-contrast telescope designs with apertures up to 100 m have been proposed for the purpose of rocky exoplanet mapping: for example, the 25-m interferometric telescope Exo-Life Finder (ELF; Kuhn et al. 2018; Berdyugina et al. 2018), and the 100-m OWL-Moon telescope on the Moon (Schneider et al. 2022), among others.

Most recently, design studies have been initiated for the NASA space-based Habitable Worlds Observatory (HWO) with aperture up to 8 m (see Lagage et al. 2026, this topical collection for a detailed discussion). The design of HWO aims to achieve at least the 10^{-10} contrast at angular separations corresponding to the habitable zones of nearby solar-type stars, using stellar coronagraphy and multiple differential techniques including spectroscopy and polarimetry. Achieving such a high imaging contrast will open a unique opportunity for obtaining multi-spectral albedo maps of temperate rocky exoplanets and detecting photosynthetic life in the solar neighbourhood (Berdyugina et al. 2025). HWO science case studies and scientific requirements provide estimates of possible number of detections and exposure times necessary to achieve these and other scientific goals of the HWO mission.

5 Conclusion: On the Prevalence of Water Versus Land Planets

This review has demonstrated how the water/land ratio on a temperate planet is an intricate outcome of internal mantle dynamics. In turn, oceans trade off with land surfaces to exert a grand influence on climates and biospheres. One might legitimately ask whether Earth's balanced water/land ratio is a coincidence, which could possibly augment the attributes that have been posited to make Earth a rare planet (e.g., Scherf et al. 2024, see also Spohn et al. 2026, this topical collection), or whether the ratio is a natural outcome of planetary processes. There is no definitive answer to this question yet, but we have the tools to approach it. We consider three ingredients that were previously discussed, noting that there is no evidence for these ingredients requiring plate tectonics in order to perform their functional purpose, although recycling in a mobile-lid mode may enable ingredient 3 especially.

First, to keep dry land above sea level, the planet must support substantial surface topography. Conveniently, there are many ways to create this topography. Although Earth's elevation profile is undoubtedly complex, the product of billions of years of plate movement and mountain-building, large-scale flows in the mantle will nonetheless express themselves as long-wavelength dynamic topography at the surface. All convecting rocky planets thus have some intrinsic topography.

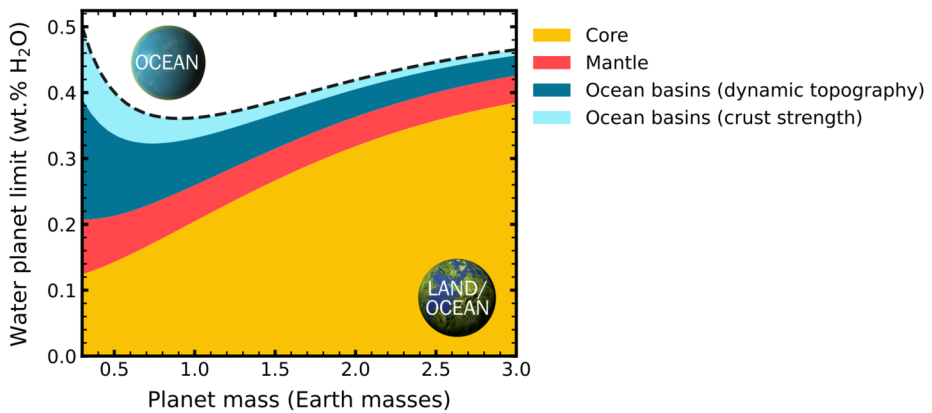


Fig. 7 The minimum bulk water mass fraction required to completely cover a planet in oceans. Coloured swaths represent the contribution to this water capacity of each of the planet's main water reservoirs, while the dashed line shows the sum of all reservoirs. Water mass fractions above the dashed line would likely make a water planet with no dry land. Ocean basin capacities assume purely-dynamic topography (dark blue contribution), plus the possibility of additional topography (light blue contribution) capped at where gravity exceeds a crust strength of 100 MPa (Guimond et al. 2022). Mantle water content at water saturation (red contribution) is the median from Guimond et al. (2023), assuming a solidified mantle with water stored only in nominally anhydrous minerals at a conservative potential temperature of 1600 K. Core water content (yellow contribution) is solved iteratively using the parameterisation for metal-silicate partitioning of H_2O from Luo et al. (2024) given the mantle plus surface water mass above (i.e., assuming no loss to space), which depends on the water concentration in the core and on pressure (taken to be half the core-mantle boundary pressure), and is qualitatively similar to Li et al. (2020). Core mass fraction is assumed to be 32.5%

Less certain beyond Earth, but potentially dramatic in shaping ocean basins, is the isostatic flotation of low-density felsic 'continents' above the denser mafic crust that progenates them. The formation of continental crust is related to the water cycle between the mantle and the surface, at least in the context of modern plate tectonics (e.g., Hönig and Spohn 2023), but may also matter for tectonic modes that may have dominated Earth during the Hadean and Archean. Unfortunately, the rock record is sparse for these periods and the early volume of continental crust (compare Fig. 3) and the mechanism(s) of their formation and growth are still uncertain (e.g., Cawood et al. 2022; Chowdhury et al. 2025; Rey et al. 2024).

At finer scales, a number of other surface processes are known to 'roughen' one-plate planets in the Solar System: lava doming, impact cratering, chemical dissolution of the crust, or any means of tectonic extension or compression, for example. Regardless of how topography is generated, however, gravity will ultimately cap its maximum prominence due to finite lithospheric strength, such that Earth-size planets likely do not support mountains surpassing 10 km (Melosh 2011; Guimond et al. 2022). Nevertheless, the large scope for planetary topography at all scales suggests that we can nevertheless expect environments where liquid water, if present, can at least pond if not form deep oceans.

Second, it is essential that the bulk planet water inventory is sufficiently small to preclude oceans tens to hundreds of kilometres deep. For an estimate of how the upper limit on this water mass fraction scales with planet mass, we add ocean basin capacity scalings for topography (Guimond et al. 2022) on top of water-saturated solid mantles (Guimond et al. 2023) and pressure-dependent H_2O partitioning into the core (Luo et al. 2024). The resulting 'water planet limit' in terms of planet mass fraction increases with planet mass, but stays safely below 1 wt.% (Fig. 7). The largest uncertainties on an appropriate bulk water mass fraction limit lie in the capacities of the metallic-iron core and the perovskite lower mantle to

sequester water. These saturation limits depend on the total core and mantle masses, as well as on their temperatures. (Unknown) water hidden in the core is nonetheless less relevant for water on the surface. We conclude that on temperate planets with solidified mantles, bulk water contents of more than half a percent water by mass may prohibit dry land, based on the limited capacities of these planets' interiors and ocean basins to contain water,¹⁵ in agreement with Scherf et al. (2024). Accretion within the snowline (e.g., Tian and Ida 2015; Lichtenberg et al. 2021) could be important in keeping water mass fractions below this limit.

Considering such dry yet not dessicated planets, we can compare ocean basin capacities with water outgassing rates to speculate on the prevalence of ocean and desert worlds conservatively. If dynamic topography represents the minimum 'intrinsic' ocean basin capacity, then absent any other topography an Earth-mass planet would flood under $\mathcal{O}(0.1)$ ocean masses (Guimond et al. 2022). Meanwhile, volcanic outgassing rates of water can be up to $\mathcal{O}(0.1)$ ocean masses per Gyr on oxidised stagnant lid planets (see Table 1), but also as low as $\mathcal{O}(0.001)$ ocean masses per Gyr under certain conditions. Peak singular episodes of water degassing seem to occur in the late stages of magma ocean crystallisation (e.g., Hamano et al. 2013; Salvador et al. 2017). Unless a temperate rocky exoplanet has retained a bulk silicate water mass fraction of only $<10^{-4}$ from formation or its volcanic outgassing is extremely inefficient, and assuming steam can condense, it is plausible that its ocean basins will be filled by the time we observe it.

The comparison above highlights the need for the third ingredient: the existence of feedback mechanisms that regulate sea level. Water exchange between surface and interior may be governed by the pressure dependence of water solubility in magma, which regulates degassing at the seafloor (e.g., Rüpke and Gaillard 2024). Rates of outgassing and ingassing are also subject to the effect of water on decreasing both the viscosity and the solidus temperature of mantle rock (e.g., Sandu et al. 2011; Seales and Lenardic 2020). Within the paradigm of plate tectonics, it is noteworthy that both the primary loci of water subduction and degassing are arc-related subduction zones, such that stable equilibrium states exist when the length of subduction zones is either minimised or maximised (Höning and Spohn 2023), Earth's balanced land/water ratio being close to the latter.

Geochemical data suggest that the early continents were flooded, with low relief (Rey et al. 2024). Planet cooling and ocean crust subsidence may then have led to the rise of the continents. Plate tectonics, operating since at least the Proterozoic, may have stabilized the surface water inventory, as evidenced by the long-term constancy of the freeboard. In any case, too little is known about the early Earth to suggest a simple or universal mechanism that would result in a balanced water/land distribution.

Clues to the possibilities raised throughout this article may ultimately be found on rocky exoplanets. A diversity of various water/land scenarios can be unveiled through indirect imaging of planetary surfaces using advanced multi-colour inversions of reflected light-curves (e.g., Berdyugina and Kuhn 2019; Kawahara 2020), if suitable data is delivered by the planned large-aperture and high-contrast telescopes on the ground and in space, such as the ELT and HWO. By determining water/land ratios on rocky exoplanets, we will start to see whether 'intermediate', Earth-like ratios exist on other worlds, hence whether water is safely delivered to and retained on these planets, and whether their deep water cycles exhibit the self-regulation to keep such a balance.

¹⁵Caveats abound to this simplified analysis; for example, very large masses of primordial water may enter the core during differentiation, and the associated large masses in the magma ocean are subsequently lost to space.

Acknowledgements CMG is supported by the UK Science and Technology Facilities Council [grant number ST/W000903/1]. PAC acknowledges support from Australian Research Council grant FL160100168. Two anonymous reviewers have provided feedback which has improved this manuscript. CMG thanks Michael Way, Tad Komacek, Rob Spaargaren, Josh Krissansen-Totton, Harrison Nicholls, and Rob Law for additional feedback and clarification.

Declarations

Competing Interests The authors declare no competing interests.

Open Access This article is licensed under a Creative Commons Attribution 4.0 International License, which permits use, sharing, adaptation, distribution and reproduction in any medium or format, as long as you give appropriate credit to the original author(s) and the source, provide a link to the Creative Commons licence, and indicate if changes were made. The images or other third party material in this article are included in the article's Creative Commons licence, unless indicated otherwise in a credit line to the material. If material is not included in the article's Creative Commons licence and your intended use is not permitted by statutory regulation or exceeds the permitted use, you will need to obtain permission directly from the copyright holder. To view a copy of this licence, visit <http://creativecommons.org/licenses/by/4.0/>.

References

- Agol E, Dorn C, Grimm SL, et al (2021) Refining the transit-timing and photometric analysis of TRAPPIST-1: masses, radii, densities, dynamics, and ephemerides. *Planet Sci J* 2(1):1. <https://doi.org/10.3847/PSJ/abd022>
- Aizawa M, Kawahara H, Fan S (2020) Global mapping of an exo-Earth using sparse modeling. *Astrophys J* 896:22. <https://doi.org/10.3847/1538-4357/ab8d30>
- Alexander CMO, Bowden R, Fogel ML, et al (2012) The provenances of asteroids, and their contributions to the volatile inventories of the terrestrial planets. *Science* 337(6095):721–723. <https://doi.org/10.1126/science.1223474>
- Anbar AD, Knoll AH (2002) Proterozoic ocean chemistry and evolution: a bioinorganic bridge? *Science* 297(5584):1137–1143. <https://doi.org/10.1126/science.1069651>
- Anderson RC, Dohm JM, Golombek MP, et al (2001) Primary centers and secondary concentrations of tectonic activity through time in the western hemisphere of Mars. *J Geophys Res Planets* 106(E9):20563–20585. <https://doi.org/10.1029/2000JE001278>
- Andrews-Hanna JC, Zuber MT, Banerdt WB (2008) The Borealis basin and the origin of the Martian crustal dichotomy. *Nature* 453(7199):1212–1215. <https://doi.org/10.1038/nature07011>
- Armstrong RL (1981) Radiogenic isotopes: the case for crustal recycling on a near-steady-state non-continental-growth Earth. *Philos Trans R Soc Lond Ser A, Math Phys Sci* 301(1461):443–472. <https://doi.org/10.1098/rsta.1981.0122>
- Arnould M, Coltice N, Flament N, et al (2018) On the scales of dynamic topography in whole-mantle convection models. *Geochem Geophys Geosyst* 19(9):3140–3163
- Arnscheidt CW, Rothman DH (2022) Presence or absence of stabilizing Earth system feedbacks on different time scales. *Sci Adv* 8(46):eadc9241. <https://doi.org/10.1126/sciadv.adc9241>
- Arp TB, Kistner-Morris J, Aji V, et al (2020) Quieting a noisy antenna reproduces photosynthetic light-harvesting spectra. *Science* 368(6498):1490–1495. <https://doi.org/10.1126/science.aba6630>
- Asensio Ramos A, Pallé E (2021) Planet cartography with neural learned regularization. *Astron Astrophys* 646:A4. <https://doi.org/10.1051/0004-6361/202040066>
- Awramik SM, McNamara KJ (2007) The evolution and diversification of life. In: Sullivan WT III, Baross JA (eds) *Planets and life*, vol 9. Cambridge University Press, Cambridge, pp 313–334
- Bada JL (2004) How life began on Earth: a status report. *Earth Planet Sci Lett* 226(1–2):1–15. <https://doi.org/10.1016/j.epsl.2004.07.036>
- Baker VR, Strom RG, Gulick VC, et al (1991) Ancient oceans, ice sheets and the hydrological cycle on Mars. *Nature* 352(6336):589–594. <https://doi.org/10.1038/352589a0>
- Balbi A, Frank A (2024) The oxygen bottleneck for technospheres. *Nat Astron* 8:39–43. <https://doi.org/10.1038/s41550-023-02112-8>. [arXiv:2308.01160](https://arxiv.org/abs/2308.01160) [astro-ph.EP]
- Bandfield JL, Hamilton VE, Christensen PR, et al (2004) Identification of quartzofeldspathic materials on Mars. *J Geophys Res Planets* 109(E10). <https://doi.org/10.1029/2004JE002290>

- Bar-On YM, Phillips R, Milo R (2018) The biomass distribution on Earth. *Proc Natl Acad Sci USA* 115(25):6506–6511. <https://doi.org/10.1073/pnas.1711842115>
- Barnes R (2017) Tidal locking of habitable exoplanets. *Celest Mech Dyn Astron* 129(4):509–536. <https://doi.org/10.1007/s10569-017-9783-7>
- Baross JA, Hoffman SE (1985) Submarine hydrothermal vents and associated gradient environments as sites for the origin and evolution of life. *Orig Life Evol Biosph* 15(4):327–345. <https://doi.org/10.1007/BF01808177>
- Barrell J (1914) The strength of the Earth's crust. *J Geol* 22(7):655–683
- Barrett TJ, Bryson JFJ, Geraki K (2025) The source of hydrogen in Earth's building blocks. *Icarus* 436:116588. <https://doi.org/10.1016/j.icarus.2025.116588>
- Baumeister P, Miozzi F, Guimond CM, et al (2025) Fundamentals of Interior Modelling and Challenges in the Interpretation of Observed Rocky Exoplanets. *Space Science Reviews* 221(8):123. <https://doi.org/10.1007/s11214-025-01248-5>
- Begg G, Griffin W, Natapov L, et al (2009) The lithospheric architecture of Africa: seismic tomography, mantle petrology, and tectonic evolution. *Geosphere* 5(1):23–50. <https://doi.org/10.1130/GES00179.1>
- Bercovici D, Karato SI (2003) Whole-mantle convection and the transition-zone water filter. *Nature* 425(6953):39–44
- Bercovici D, Schubert G, Zebib A (1988) Geoid and topography for infinite Prandtl number convection in a spherical shell. *J Geophys Res, Solid Earth* 93(B6):6430–6436
- Berdyugina SV, Kuhn JR (2019) Surface imaging of Proxima b and other exoplanets: Albedo maps, biosignatures, and technosignatures. *Astron J* 158:246. <https://doi.org/10.3847/1538-3881/ab2df3>
- Berdyugina SV, Kuhn JR, Harrington DM, et al (2016) Remote sensing of life: polarimetric signatures of photosynthetic pigments as sensitive biomarkers. *Int J Astrobiol* 15(1):45–56. <https://doi.org/10.1017/S1473550415000129>
- Berdyugina SV, Kuhn JR, Langlois M, et al (2018) The Exo-Life Finder (ELF) telescope: new strategies for direct detection of exoplanet biosignatures and technosignatures. In: Marshall HK, Spyromilio J (eds) *Ground-based and Airborne Telescopes VII*, p 107004I. <https://doi.org/10.1117/12.2313781>
- Berdyugina SV, Kuhn JR, Belikov R, et al (2019) In: *Exoplanet terra incognita*. Springer, Cham, pp 337–351. https://doi.org/10.1007/978-3-319-62849-3_20
- Berdyugina S, Patty L, Grone J, et al (2025) Detecting alien living worlds and photosynthetic life using imaging polarimetry with the HWO coronagraph. In: Lee JC, Noviello J, LaMassa S, Postman M (eds) *Towards the habitable worlds observatory: visionary science and transformational technology*. ASP conf ser. <https://doi.org/10.48550/arXiv.2507.03819>. [arXiv:2507.03819](https://arxiv.org/abs/2507.03819) [astro-ph.EP]
- Biersteker JB, Schlichting HE (2020) Losing oceans: the effects of composition on the thermal component of impact-driven atmospheric loss. *Mon Not R Astron Soc* 501(1):587–595. <https://doi.org/10.1093/mnras/staa3614>. [arXiv:2007.01446](https://arxiv.org/abs/2007.01446) [astro-ph]
- Bodnar RJ, Azbej T, Becker SP, et al (2013) Whole Earth geohydrologic cycle, from the clouds to the core: the distribution of water in the dynamic Earth system. *Spec Pap, Geol Soc Am* 500:431–461
- Bolfan-Casanova N (2005) Water in the Earth's mantle. *Mineral Mag* 69(3):229–257. <https://doi.org/10.1180/0026461056930248>
- Bolfan-Casanova N, Keppeler H, Rubie DC (2003) Water partitioning at 660 km depth and evidence for very low water solubility in magnesium silicate perovskite. *Geophysical Research Letters* 30(17). <https://doi.org/10.1029/2003GL017182>
- Bower DJ, Hakim K, Sossi PA, et al (2022) Retention of water in terrestrial magma oceans and carbon-rich early atmospheres. *Planet Sci J* 3(4):93. <https://doi.org/10.3847/PSJ/ac5fb1>
- Brachmann C, Noack L, Baumeister PA, et al (2025) Distinct types of C-H-O-N atmospheres and surface pressures depending on melt redox state and outgassing efficiency. *Icarus* 429:116450. <https://doi.org/10.1016/j.icarus.2024.116450>
- Brantley SL, Shaughnessy A, Lebedeva MI, et al (2023) How temperature-dependent silicate weathering acts as Earth's geological thermostat. *Science* 379(6630):382–389. <https://doi.org/10.1126/science.add2922>
- Bristow LA, Mohr W, Ahmerkamp S, et al (2017) Nutrients that limit growth in the ocean. *Curr Biol* 27(11):R474–R478. <https://doi.org/10.1016/j.cub.2017.03.030>
- Brugman K, Phillips MG, Till CB (2021) Experimental determination of mantle solidi and melt compositions for two likely rocky exoplanet compositions. *J Geophys Res Planets* 126(7):e2020JE006731. <https://doi.org/10.1029/2020JE006731>
- Buie MW, Young EF, Binzel RP (1997) Surface appearance of Pluto and Charon. In: Stern SA, Tholen DJ (eds) *Pluto and Charon*. p 269
- Bureau H, Keppeler H (1999) Complete miscibility between silicate melts and hydrous fluids in the upper mantle: experimental evidence and geochemical implications. *Earth Planet Sci Lett* 165(2):187–196. [https://doi.org/10.1016/S0012-821X\(98\)00266-0](https://doi.org/10.1016/S0012-821X(98)00266-0)

- Burgess MG, Gaines SD (2018) The scale of life and its lessons for humanity. *Proc Natl Acad Sci USA* 115(25):6328–6330. <https://doi.org/10.1073/pnas.1807019115>
- Burkhardt C, Spitzer F, Morbidelli A, et al (2021) Terrestrial planet formation from lost inner Solar System material. *Sci Adv* 7(52):eabj7601. <https://doi.org/10.1126/sciadv.abj7601>
- Byrne PK, Klimczak C, Celâl Şengör AM, et al (2014) Mercury's global contraction much greater than earlier estimates. *Nat Geosci* 7:301–307. <https://doi.org/10.1038/ngeo2097>
- Byrne PK, Ghail RC, Gilmore MS, et al (2020) Venus tesserae feature layered, folded, and eroded rocks. *Geology* 49(1):81–85. <https://doi.org/10.1130/G47940.1>
- Campbell IH, Taylor SR (1983) No water, no granites-no oceans, no continents. *Geophys Res Lett* 10(11):1061–1064
- Carbognani A, Tanga P, Cellino A, et al (2012) The representation of asteroid shapes: a test for the inversion of Gaia photometry. *Planet Space Sci* 73(1):80–85. <https://doi.org/10.1016/j.pss.2011.12.002>. arXiv:1903.12633 [astro-ph.EP]
- Cassata WS (2025) A refined isotopic composition of cometary xenon and implications for the accretion of comets and carbonaceous chondrites on Earth. *Earth Planet Sci Lett* 660:119307. <https://doi.org/10.1016/j.epsl.2025.119307>
- Catling DC, Glein CR, Zahnle KJ, et al (2005) Why O₂ is required by complex life on habitable planets and the concept of planetary “oxygenation time”. *Astrobiology* 5(3):415–438. <https://doi.org/10.1089/ast.2005.5.415>
- Cawood PA, Hawkesworth CJ (2019) Continental crustal volume, thickness and area, and their geodynamic implications. *Gondwana Res* 66:116–125
- Cawood P, Hawkesworth C, Dhuime B (2013) The continental record and the generation of continental crust. *GSA Bull* 125(1–2):14–32. <https://doi.org/10.1130/B30722.1>
- Cawood PA, Chowdhury P, Mulder JA, et al (2022) Secular evolution of continents and the Earth system. *Rev Geophys* 60(4):e2022RG000789. <https://doi.org/10.1029/2022RG000789>
- Champagnac JD, Schlunegger F, Norton K, et al (2009) Erosion-driven uplift of the modern Central Alps. *Tectonophysics* 474(1):236–249. <https://doi.org/10.1016/j.tecto.2009.02.024>
- Chandler MA, Sohl LE (2000) Climate forcings and the initiation of low-latitude ice sheets during the Neoproterozoic Varanger glacial interval. *J Geophys Res, Atmos* 105(D16):20737–20756. <https://doi.org/10.1029/2000JD900221>
- Chang YY, Hsieh WP, Tan E, et al (2017) Hydration-reduced lattice thermal conductivity of olivine in Earth's upper mantle. *Proc Natl Acad Sci USA* 114(16):4078–4081
- Chen K, Rudnick RL, Wang Z, et al (2020) How mafic was the Archean upper continental crust? Insights from Cu and Ag in ancient glacial diamictites. *Geochim Cosmochim Acta* 278:16–29. <https://doi.org/10.1016/j.gca.2019.08.002>
- Cheng KW, Ballantyne HA, Golabek GJ, et al (2024) Combined impact and interior evolution models in three dimensions indicate a southern impact origin of the Martian Dichotomy. *Icarus* 420:116137. <https://doi.org/10.1016/j.icarus.2024.116137>
- Chowdhury P, Cawood PA, Mulder JA (2025) Subaerial emergence of continents on Archean Earth. *Annu Rev Earth Planet Sci*. <https://doi.org/10.1146/annurev-earth-040722-093345>
- Churkina G, Running SW (1998) Contrasting climatic controls on the estimated productivity of global terrestrial biomes. *Ecosystems* 1:206–215. <https://doi.org/10.1007/s100219900016>
- Comiso J (2023) Bootstrap Sea Ice Concentrations from Nimbus-7 SMMR and DMSP SSM/I-SSMIS, Version 4. <https://doi.org/10.5067/X5L6G8MH0130>. <http://nsidc.org/data/NSIDC-0079/versions/4>
- Coogan LA, Caves Rugenstein JK (2025) Regulation of the carbon cycle on geological timescales. In: Anbar A, Weis D (eds) *Treatise on geochemistry*, 3rd edn. Elsevier, Oxford, pp 419–465. <https://doi.org/10.1016/B978-0-323-99762-1.00060-7>
- Coogan LA, Dosso SE (2015) Alteration of ocean crust provides a strong temperature dependent feedback on the geological carbon cycle and is a primary driver of the Sr-isotopic composition of seawater. *Earth Planet Sci Lett* 415:38–46. <https://doi.org/10.1016/j.epsl.2015.01.027>
- Coogan LA, Gillis KM (2013) Evidence that low-temperature Oceanic hydrothermal systems play an important role in the silicate-carbonate weathering cycle and long-term climate regulation. *Geochem Geophys Geosyst* 14(6):1771–1786. <https://doi.org/10.1002/ggge.20113>
- Coogan LA, Gillis KM (2018) Temperature dependence of chemical exchange during seafloor weathering: Insights from the Troodos ophiolite. *Geochim Cosmochim Acta* 243:24–41. <https://doi.org/10.1016/j.gca.2018.09.025>
- Corliss JB, Baross JA, Hoffman SE (1981) An hypothesis concerning the relationships between submarine hot springs and the origin of life on Earth. *Oceanol Acta. Special issue*, pp 59–69
- Cowan NB, Abbot DS (2014) Water cycling between ocean and mantle: super-earths need not be waterworlds. *Astrophys J* 781(1):27. <https://doi.org/10.1088/0004-637X/781/1/27>. arXiv:1401.0720

- Cowan NB, Fujii Y (2020) Mapping exoplanets. In: Deeg HJ, Belmonte JA (eds) Handbook of exoplanets. Springer, Cham, pp 1–18. https://doi.org/10.1007/978-3-319-30648-3_147-2
- Cowan NB, Agol E, Meadows VS, et al (2009) Alien maps of an ocean-bearing world. *Astrophys J* 700:915–923. <https://doi.org/10.1088/0004-637X/700/2/915>
- Cowan NB, Robinson T, Livengood TA, et al (2011) Rotational variability of Earth's polar regions: implications for detecting snowball planets. *Astrophys J* 731(1):76. <https://doi.org/10.1088/0004-637X/731/1/76>
- Cowan NB, Chayes V, Bouffard É, et al (2017) Odd harmonics in exoplanet photometry: weather or artifact? *Mon Not R Astron Soc* 467:747–757. <https://doi.org/10.1093/mnras/stx133>
- Czarnecki S, Hardgrove C, Gasda PJ, et al (2020) Identification and description of a silicic volcanoclastic layer in Gale Crater, Mars, using active neutron interrogation. *J Geophys Res Planets* 125(3):e2019JE006180. <https://doi.org/10.1029/2019JE006180>
- Damer B, Deamer D (2020) The hot spring hypothesis for an origin of life. *Astrobiology* 20(4):429–452. <https://doi.org/10.1089/ast.2019.2045>
- Davies DR, Ghelichkhan S, Hoggard M, et al (2023) Observations and models of dynamic topography: current status and future directions. In: Dynamics of plate tectonics and mantle convection, pp 223–269
- Deamer D, Cary F, Damer B (2022) Urability: a property of planetary bodies that can support an origin of life. *Astrobiology* 22(7):889–900. <https://doi.org/10.1089/ast.2021.0173>
- DeGuzman V, Vercootere W, Shenasa H, et al (2014) Generation of oligonucleotides under hydrothermal conditions by non-enzymatic polymerization. *J Mol Evol* 78(5):251–262. <https://doi.org/10.1007/s00239-014-9623-2>
- Del Genio AD, Kiang NY, Way MJ, et al (2019a) Albedos, equilibrium temperatures, and surface temperatures of habitable planets. *Astrophys J* 884:75. <https://doi.org/10.3847/1538-4357/ab3be8>
- Del Genio AD, Way MJ, Amundsen DS, et al (2019b) Habitable climate scenarios for Proxima Centauri b with a dynamic ocean. *Astrobiology* 19(1):99–125. <https://doi.org/10.1089/ast.2017.1760>
- Dhuime B, Wuestefeld A, Hawkesworth CJ (2015) Emergence of modern continental crust about 3 billion years ago. *Nat Geosci* 8(7):552–555. <https://doi.org/10.1038/ngeo2466>
- Djokic T, Van Kranendonk MJ, Campbell KA, et al (2017) Earliest signs of life on land preserved in ca. 3.5 ga hot spring deposits. *Nat Commun* 8. <https://doi.org/10.1038/ncomms15263>
- Dong J, Fischer RA, Stixrude LP, et al (2021) Constraining the volume of Earth's early oceans with a temperature-dependent mantle water storage capacity model. *AGU Adv* 2(1):e2020AV000323. <https://doi.org/10.1029/2020AV000323>
- Dorn C, Lichtenberg T (2021) Hidden water in magma ocean exoplanets. *Astrophys J Lett* 922(1):L4. <https://doi.org/10.3847/2041-8213/ac33af>
- Dorn C, Noack L, Rozel A (2018) Outgassing on stagnant-lid super-earths. *Astron Astrophys* 614:A18
- Dowdeswell JA, Ottesen D, Rise L (2010) Rates of sediment delivery from the Fennoscandian Ice Sheet through an ice age. *Geology* 38(1):3–6. <https://doi.org/10.1130/G25523.1>
- Edgar LA, Fedo CM, Gupta S, et al (2020) A lacustrine paleoenvironment recorded at Vera RubinRidge, Gale Crater: overview of the sedimentology and stratigraphy observed by the Mars Science Laboratory Curiosity rover. *J Geophys Res Planets* 125(3):e2019JE006307. <https://doi.org/10.1029/2019JE006307>
- Elkins-Tanton L, Smrekar S, Hess, et al (2007) Volcanism and volatile recycling on a one-plate planet: applications to Venus. *Treatise on Geophysics* 9:197–216
- Eshleman VR (1979) Gravitational lens of the sun: its potential for observations and communications over interstellar distances. *Science* 205(4411):1133–1135. <https://doi.org/10.1126/science.205.4411.1133>
- Fairchild IJ, Kennedy MJ (2007) Neoproterozoic glaciation in the Earth System. *J Geol Soc* 164(5):895–921. <https://doi.org/10.1144/0016-76492006-191>
- Fan S, Li C, Li JZ, et al (2019) Earth as an exoplanet: a two-dimensional alien map. *Astrophys J Lett* 882(1):L1. <https://doi.org/10.3847/2041-8213/ab3a49>
- Farr B, Farr WM, Cowan NB, et al (2018) Exocartographer: a Bayesian framework for mapping exoplanets in reflected light. *Astron J* 156(4):146. <https://doi.org/10.3847/1538-3881/aad775>. arXiv:1802.06805
- Feldt M, Bertram T, Correia C, et al (2024) High strehl and high contrast for the ELT instrument METIS: final design, implementation, and predicted performance of the single-conjugate adaptive optics system. *Exp Astron* 58(3):20. <https://doi.org/10.1007/s10686-024-09968-2>. arXiv:2411.17341 [astro-ph.IM]
- Field CB, Behrenfeld MJ, Randerson JT, et al (1998) Primary production of the biosphere: integrating terrestrial and Oceanic components. *Science* 281:237. <https://doi.org/10.1126/science.281.5374.237>
- Flament N (2019) Present-day dynamic topography and lower-mantle structure from palaeogeographically constrained mantle flow models. *Geophys J Int* 216(3):2158–2182
- Flament N, Gurnis M, Müller RD (2013) A review of observations and models of dynamic topography. *Lithosphere* 5(2):189–210
- Fluri DM, Berdyugina SV (2010) Orbital parameters of extrasolar planets derived from polarimetry. *Astron Astrophys* 512:A59. <https://doi.org/10.1051/0004-6361/200809970>

- Foley BJ, Driscoll PE (2016) Whole planet coupling between climate, mantle, and core: Implications for rocky planet evolution. *Geochim Geophys Geosyst* 17:1885–1914. <https://doi.org/10.1002/2015GC006210>
- Ford D, Williams PD (2013) *Karst hydrogeology and geomorphology*. Wiley, New York
- Frank EA, Meyer BS, Mojzsis SJ (2014) A radiogenic heating evolution model for cosmochemically Earth-like exoplanets. *Icarus* 243:274–286. <https://doi.org/10.1016/j.icarus.2014.08.031>
- Frost CD, Mueller PA (2024) Archean cratons: time capsules of the early Earth. *Elements* 20(3):162–167. <https://doi.org/10.2138/gselements.20.3.162>
- Fu S, Yang J, Si K, et al (2019) Water Concentration in Single-Crystal (Al,Fe)-Bearing Bridgmanite Grown From the Hydrous Melt: Implications for Dehydration Melting at the Topmost Lower Mantle. *Geophysical Research Letters* 46(17–18):10346–10357. <https://doi.org/10.1029/2019GL084630>
- Fujii Y, Kawahara H (2012) Mapping Earth analogs from photometric variability: spin-orbit tomography for planets in inclined orbits. *Astrophys J* 755(2):101. <https://doi.org/10.1088/0004-637X/755/2/101>. arXiv: 1204.3504 [astro-ph]
- Fujii Y, Kawahara H, Suto Y, et al (2010) Colors of a second Earth: estimating the fractional areas of ocean, land, and vegetation of Earth-like exoplanets. *Astrophys J* 715:866–880. <https://doi.org/10.1088/0004-637X/715/2/866>
- Fujii Y, Kawahara H, Suto Y, et al (2011) Colors of a second Earth. II. Effects of clouds on photometric characterization of Earth-like exoplanets. *Astrophys J* 738:184. <https://doi.org/10.1088/0004-637X/738/2/184>
- Fyfe WS (1978) The evolution of the Earth's crust: modern plate tectonics to ancient hot spot tectonics? *Chem Geol* 23(1):89–114. [https://doi.org/10.1016/0009-2541\(78\)90068-2](https://doi.org/10.1016/0009-2541(78)90068-2)
- Gaillard F, Scaillet B (2014) A theoretical framework for volcanic degassing chemistry in a comparative planetology perspective and implications for planetary atmospheres. *Earth Planet Sci Lett* 403:307–316. <https://doi.org/10.1016/j.epsl.2014.07.009>
- Gilmore MS, Mueller N, Helbert J (2015) VIRTIS emissivity of Alpha Regio, Venus, with implications for tessera composition. *Icarus* 254:350–361. <https://doi.org/10.1016/j.icarus.2015.04.008>
- Gislason SR, Oelkers EH, Eiriksdottir ES, et al (2008) The feedback between climate and weathering. *Mineral Mag* 72(1):317–320. <https://doi.org/10.1180/minmag.2008.072.1.317>
- Glaser D, Hartnett HE, Desch SJ, et al (2020) Detectability of life using oxygen on pelagic planets and water worlds. *Astrophys J* 893:163. <https://doi.org/10.3847/1538-4357/ab822d>
- Glaser D, Aleinov I, Leboissetier A, et al (2025) Continental orientation and the climate of land-dominated, arid planets. *Planet Sci J*. <https://doi.org/10.3847/PSJ/adccb6>
- Glaser DM, et al (2026) Euhabitability: A new term to aid in the search for life in addition to the habitable zone framework. *Space Sci Rev* 222
- Goes S, Agrusta R, van Hunen J, et al (2017) Subduction-transition zone interaction: a review. *Geosphere* 13(3):644–664. <https://doi.org/10.1130/GES01476.1>
- Golabek GJ, Keller T, Gerya TV, et al (2011) Origin of the Martian dichotomy and Tharsis from a giant impact causing massive magmatism. *Icarus* 215(1):346–357. <https://doi.org/10.1016/j.icarus.2011.06.012>
- Goodwin AM (1996) *Principles of Precambrian geology*. Academic Press, London. <https://doi.org/10.1016/B978-0-12-289770-2.X5000-6>
- Gouge TA, Mustard JF, Head JW, et al (2015) Assessing the mineralogy of the watershed and fan deposits of the Jezero crater paleolake system, Mars. *J Geophys Res Planets* 120(4):775–808. <https://doi.org/10.1002/2014JE004782>
- Graham RJ, Pierrehumbert RT (2024) Carbon cycle instability for high-CO₂ exoplanets: Implications for habitability. <https://doi.org/10.3847/1538-4357/ad45fb>. arXiv:2405.05396
- Gray JS (1997) Marine biodiversity: patterns, threats and conservation needs. *Biodivers Conserv* 6(1):153–175
- Griggs DT, Blacic JD (1965) Quartz: anomalous weakness of synthetic crystals. *Science* 147(3655):292–295. <https://doi.org/10.1126/science.147.3655.292>
- Gu L, Fan S, Li J, et al (2021) Earth as a proxy exoplanet: deconstructing and reconstructing spectrophotometric light curves. *Astron J* 161:122. <https://doi.org/10.3847/1538-3881/abd54a>
- Gu L, Zeng ZC, Fan S, et al (2022) Earth as a proxy exoplanet: simulating DSCOVR/EPIC observations using the Earth spectrum simulator. *Astron J* 163(6):285. <https://doi.org/10.3847/1538-3881/ac5e2e>
- Guillou L, Jaupart C (1995) On the effect of continents on mantle convection. *J Geophys Res, Solid Earth* 100(B12):24217–24238
- Guimond CM, Noack L, Ortenzi G, et al (2021) Low volcanic outgassing rates for a stagnant lid Archean earth with graphite-saturated magmas. *Phys Earth Planet Inter* 320:106788. <https://doi.org/10.1016/j.pepi.2021.106788>

- Guimond CM, Rudge JF, Shorttle O (2022) Blue marble, stagnant lid: could dynamic topography avert a waterworld? *Planet Sci J* 3(3):66. <https://doi.org/10.3847/PSJ/ac562e>
- Guimond CM, Shorttle O, Rudge JF (2023) Mantle mineralogy limits to rocky planet water inventories. *Mon Not R Astron Soc* 521(2):2535–2552. <https://doi.org/10.1093/mnras/stad148>
- Guo M, Korenaga J (2020) Argon constraints on the early growth of felsic continental crust. *Sci Adv* 6(21):eaz6234
- Guthnick P (1906) Resultate aus photometrischen Beobachtungen der sechs helleren Saturntrabanten. *Astron Nachr* 171(18):273. <https://doi.org/10.1002/asna.19061711802>
- Hakim K, Bower DJ, Tian M, et al (2021) Lithologic controls on silicate weathering regimes of temperate planets. *Planet Sci J* 2(2):49
- Hamano K, Abe Y, Genda H (2013) Emergence of two types of terrestrial planet on solidification of magma ocean. *Nature* 497(7451):607–610. <https://doi.org/10.1038/nature12163>
- Hao J, Knoll AH, Huang F, et al (2020) Cycling phosphorus on the Archean Earth: part II. Phosphorus limitation on primary production in Archean ecosystems. *Geochim Cosmochim Acta* 280:360–377. <https://doi.org/10.1016/j.gca.2020.04.005>
- Harding S, Margulis L (2009) Water Gaia: 3.5 thousand million years of wetness on planet Earth. In: Crist E, Rinker H (eds) *Gaia in turmoil*. MIT Press, Cambridge, pp 41–60
- Harte J (2011) *Maximum entropy and ecology: a theory of abundance, distribution, and energetics*. Oxford series in ecology and evolution. Oxford University Press, Cambridge
- Hartogh P, Lis DC, Bockelée-Morvan D, et al (2011) Ocean-like water in the Jupiter-family comet 103P/Hartley 2. *Nature* 478(7368):218–220. <https://doi.org/10.1038/nature10519>
- Hashimoto GL, Roos-Serote M, Sugita S, et al (2008) Felsic highland crust on Venus suggested by Galileo Near-Infrared Mapping Spectrometer data. *J Geophys Res Planets* 113(E5). <https://doi.org/10.1029/2008JE003134>
- Hasterok D, Halpin JA, Collins AS, et al (2022) New maps of global geological provinces and tectonic plates. *Earth-Science Reviews* 231:104069. <https://doi.org/10.1016/j.earscirev.2022.104069>
- Hatton IA, McCann KS, Fryxell JM, et al (2015) The predator-prey power law: biomass scaling across terrestrial and aquatic biomes. *Science* 349(6252):aac6284. <https://doi.org/10.1126/science.aac6284>
- Heller R, Armstrong J (2014) Superhabitable worlds. *Astrobiology* 14(1):50–66. <https://doi.org/10.1089/ast.2013.1088>. [arXiv:1401.2392](https://arxiv.org/abs/1401.2392) [astro-ph.EP]
- Hirth G, Kohlstedt D (2003) Rheology of the upper mantle and the mantle wedge: a view from the experimentalists. *Geophys Monogr* 138:83–106
- Hoggard M, Austermann J, Randel C, et al (2021) Observational estimates of dynamic topography through space and time. In: *Mantle convection and surface expressions*, pp 371–411
- Höning D, Spohn T (2016) Continental growth and mantle hydration as intertwined feedback cycles in the thermal evolution of Earth. *Phys Earth Planet Inter* 255:27–49. <https://doi.org/10.1016/j.pepi.2016.03.010>
- Höning D, Spohn T (2023) Land fraction diversity on Earth-like planets and implications for their habitability. *Astrobiology* 23(4):372–394. <https://doi.org/10.1089/ast.2022.0070>
- Höning D, Hansen-Goos H, Airo A, et al (2014) Biotic vs. abiotic Earth: a model for mantle hydration and continental coverage. *Planet Space Sci* 98:5–13. <https://doi.org/10.1016/j.pss.2013.10.004>
- Houge A, Krijt S, Banzatti A, et al (2025) Smuggling unnoticed: Towards a 2D view of water and dust delivery to the inner regions of protoplanetary discs. <https://doi.org/10.48550/arXiv.2501.05881>. [arXiv:2501.05881](https://arxiv.org/abs/2501.05881)
- Hsieh WP, Ishii T, Chao KH, et al (2020) Spin transition of iron in δ -(al, fe) ooh induces thermal anomalies in Earth's lower mantle. *Geophys Res Lett* 47(4):e2020GL087036
- Hu Y, Yang J (2014) Role of ocean heat transport in climates of tidally locked exoplanets around M dwarf stars. *Proc Natl Acad Sci USA* 111:629–634. <https://doi.org/10.1073/pnas.1315215111>
- Ikoma M, Genda H (2006) Constraints on the mass of a habitable planet with water of nebular origin. *Astrophys J* 648(1):696. <https://doi.org/10.1086/505780>
- Inoue T, Wada T, Sasaki R, et al (2010) Water partitioning in the Earth's mantle. *Phys Earth Planet Inter* 2183:245–251
- Ito A (2011) A historical meta-analysis of global terrestrial net primary productivity: are estimates converging? *Glob Change Biol* 17(10):3161–3175. <https://doi.org/10.1111/j.1365-2486.2011.02450.x>
- Ito E, Harris DM, Anderson AT (1983) Alteration of Oceanic crust and geologic cycling of chlorine and water. *Geochim Cosmochim Acta* 47(9):1613–1624. [https://doi.org/10.1016/0016-7037\(83\)90188-6](https://doi.org/10.1016/0016-7037(83)90188-6)
- Ivanov MA, Head JW (2011) Global geological map of Venus. *Planet Space Sci* 59(13):1559–1600. <https://doi.org/10.1016/j.pss.2011.07.008>
- Jacobsen SD, van der Lee S (ed) (2006) *Earth's deep water cycle*, vol 168. American Geophysical Union, Washington. <https://doi.org/10.1029/GM168>

- Jarrard RD (2003) Subduction fluxes of water, carbon dioxide, chlorine, and potassium. *Geochem Geophys Geosyst* 4(5)
- Javoy M (1995) The integral enstatite chondrite model of the Earth. *Geophys Res Lett* 22(16):2219–2222. <https://doi.org/10.1029/95GL02015>
- Jellinek AM, Lenardic A, Pierrehumbert RT (2020) Ice, fire, or fizzle: the climate footprint of Earth's super-continental cycles. *Geochem Geophys Geosyst* 21:e08464. <https://doi.org/10.1029/2019GC008464>
- Jiang JH, Zhai AJ, Herman J, et al (2018) Using deep space climate observatory measurements to study the Earth as an exoplanet. *Astron J* 156(1):26. <https://doi.org/10.3847/1538-3881/aac6e2>
- Judd EJ, Tierney JE, Lunt DJ, et al (2024) A 485-million-year history of Earth's surface temperature. *Science* 385(6715):eadk3705. <https://doi.org/10.1126/science.adk3705>
- Kaasalainen M, Lamberg L, Lumme K, et al (1992) Interpretation of lightcurves of atmosphereless bodies. I - General theory and new inversion schemes. *Astron Astrophys* 259(1):318–332
- Karato SI (2011) Water distribution across the mantle transition zone and its implications for global material circulation. *Earth Planet Sci Lett* 301(3–4):413–423
- Karato SI (2015) Water in the evolution of the Earth and other terrestrial planets. In: Stevenson D, Schubert G (eds) *Treatise on geophysics*, 2nd edn. vol 9. Elsevier, New York, pp 105–144
- Karato SI, Jung H (2003) Effects of pressure on high-temperature dislocation creep in olivine. *Philos Mag* 83:401–414. <https://doi.org/10.1080/0141861021000025829>
- Karato SI, Karki B, Park J (2020) Deep mantle melting, global water circulation and its implications for the stability of the ocean mass. *Prog Earth Planet Sci* 7(1):76. <https://doi.org/10.1186/s40645-020-00379-3>
- Karlsen KS, Conrad CP, Magni V (2019) Deep water cycling and sea level change since the breakup of pangea. *Geochem Geophys Geosyst* 20(6):2919–2935
- Kawahara H (2020) Global mapping of the surface composition on an exo-Earth using color variability. *Astrophys J* 894:58. <https://doi.org/10.3847/1538-4357/ab87a1>
- Kawahara H, Fujii Y (2011) Mapping clouds and terrain of Earth-like planets from photometric variability: demonstration with planets in face-on orbits. *Astrophys J* 739(2):L62. <https://doi.org/10.1088/2041-8205/739/2/L62>. [arXiv:1106.0136](https://arxiv.org/abs/1106.0136) [astro-ph]
- Kawahara H, Masuda K (2020) Bayesian dynamic mapping of an exo-Earth from photometric variability. *Astrophys J* 900:48. <https://doi.org/10.3847/1538-4357/aba95e>
- Kelkar S, Saxena P, Kopparapu R, et al (2025) Earth as an exoplanet: investigating the effects of cloud variability on the direct-imaging of atmospheres. *Planet Sci J* 6(4):87. <https://doi.org/10.3847/PSJ/adbe7f>
- Keppler H, Ohtani E, Yang X (2024) The subduction of hydrogen: deep water cycling, induced seismicity, and plate tectonics. *Elements* 20(4):229–234
- Kiang NY, Segura A, Tinetti G, et al (2007a) Spectral signatures of photosynthesis. II. Coevolution with other stars and the atmosphere on extrasolar worlds. *Astrobiology* 7(1):252–274. <https://doi.org/10.1089/ast.2006.0108>
- Kiang NY, Siefert J, Govindjee, et al (2007b) Spectral signatures of photosynthesis. I. Review of Earth organisms. *Astrobiology* 7(1):222–251. <https://doi.org/10.1089/ast.2006.0105>
- Kiefer WS, Filiberto J, Sandu C, et al (2015) The effects of mantle composition on the peridotite solidus: implications for the magmatic history of Mars. *Geochim Cosmochim Acta* 162:247–258. <https://doi.org/10.1016/j.gca.2015.02.010>
- Kimura T, Ikoma M (2020) Formation of aqua planets with water of nebular origin: effects of water enrichment on the structure and mass of captured atmospheres of terrestrial planets. *Mon Not R Astron Soc* 496(3):3755–3766. <https://doi.org/10.1093/mnras/staa1778>
- Kimura T, Ikoma M (2022) Predicted diversity in water content of terrestrial exoplanets orbiting M dwarfs. *Nat Astron* 6(11):1296–1307. <https://doi.org/10.1038/s41550-022-01781-1>
- Kite ES, Barnett MN (2020) Exoplanet secondary atmosphere loss and revival. *Proc Natl Acad Sci USA* 117(31):18264–18271. <https://doi.org/10.1073/pnas.2006177117>
- Kite ES, Schaefer L (2021) Water on hot rocky exoplanets. *Astrophys J Lett* 909(2):L22. <https://doi.org/10.3847/2041-8213/abe7dc>. [arXiv:2103.07753](https://arxiv.org/abs/2103.07753) [astro-ph]
- Kite ES, Manga M, Gaidos E (2009) Geodynamics and rate of volcanism on massive Earth-like planets. *Astrophys J* 700(2):1732–1749. <https://doi.org/10.1088/0004-637X/700/2/1732>. [arXiv:0809.2305](https://arxiv.org/abs/0809.2305)
- Knoll AH (1985) The Precambrian evolution of terrestrial life. In: Papagiannis MD (ed) *The search for extraterrestrial life: recent developments*, IAU Symposium, vol 112. Springer, Dordrecht, pp 201–211
- Komacek TD, Abbot DS (2016) Effect of surface-mantle water exchange parameterizations on exoplanet ocean depths. *Astrophys J* 832(1):54. <https://doi.org/10.3847/0004-637X/832/1/54>
- Korenaga J (2021a) Hadean geodynamics and the nature of early continental crust. *Precambrian Res* 359:106178
- Korenaga J (2021b) Was there land on the early Earth? *Life* 11(11):1142
- Kral Q, Huet P, Bergez-Casalou C, et al (2024) An impact-free mechanism to deliver water to terrestrial planets and exoplanets. <https://doi.org/10.48550/arXiv.2412.01409>. [arXiv:2412.01409](https://arxiv.org/abs/2412.01409)

- Krissansen-Totton J, Fortney JJ (2022) Predictions for observable atmospheres of trappist-1 planets from a fully coupled atmosphere-interior evolution model. *Astrophys J* 933(1):115. <https://doi.org/10.3847/1538-4357/ac69cb>. arXiv:2207.04164 [astro-ph]
- Krissansen-Totton J, Arney GN, Catling DC (2018) Constraining the climate and ocean pH of the early Earth with a geological carbon cycle model. *Proc Natl Acad Sci USA* 115(16):4105–4110. <https://doi.org/10.1073/pnas.1721296115>
- Krissansen-Totton J, Galloway ML, Wogan N, et al (2021) Waterworlds probably do not experience magmatic outgassing. *Astrophys J* 913(2):107
- Krissansen-Totton J, Wogan N, Thompson M, et al (2024) The erosion of large primary atmospheres typically leaves behind substantial secondary atmospheres on temperate rocky planets. *Nat Commun* 15(1):8374. <https://doi.org/10.1038/s41467-024-52642-6>
- Kubyskhina D, Way MJ, Dandouras I, et al (2026) The upper atmosphere: a window into exoplanet volatile loss. *Space Sci Rev* 222
- Kuhn JR, Berdyugina SV, Capsal JF, et al (2018) The Exo-Life Finder Telescope (ELF): design and beam synthesis concepts. In: Marshall HK, Spyromilio J (eds) *Ground-based and Airborne Telescopes VII*, p 1070015. <https://doi.org/10.1117/12.2312779>
- Kuwata A, Kawahara H, Aizawa M, et al (2022) Global Mapping of Surface Composition on an Exo-Earth Using Sparse Modeling. arXiv:2204.01996 [astro-ph]
- Laakso TA, Schrag DP (2018) Limitations on limitation. *Glob Biogeochem Cycles* 32(3):486–496. <https://doi.org/10.1002/2017GB005832>
- Lagage P-O, Mandell A, Giménez A, et al (2026) The future of rocky worlds exploration. *Space Sci Rev* 222
- Le Stunff Y, Ricard Y (1995) Topography and geoid due to lithospheric mass anomalies. *Geophys J Int* 122(3):982–990
- Lebrun T, Massol H, Chassefière E, et al (2013) Thermal evolution of an early magma ocean in interaction with the atmosphere. *J Geophys Res Planets* 118(6):1155–1176
- Lecointe J (2018) Continuous reorientation of synchronous terrestrial planets due to mantle convection. *Nat Geosci* 11(3):168–172. <https://doi.org/10.1038/s41561-018-0071-2>
- Lee CT, Keller D, Dasgupta R, et al (2025) Crustal thickness effects on chemical differentiation and hydrology on Mars. *Earth Planet Sci Lett* 651:119155. <https://doi.org/10.1016/j.epsl.2024.119155>
- Léger A, Selsis F, Sotin C, et al (2004) A new family of planets? “ocean-planets”. *Icarus* 169(2):499–504. <https://doi.org/10.1016/j.icarus.2004.01.001>
- Lenardic A (2018) The diversity of tectonic modes and thoughts about transitions between them. *Philos Trans R Soc A, Math Phys Eng Sci* 376(2132):20170416. <https://doi.org/10.1098/rsta.2017.0416>
- Lenardic A, Moresi L, Jellinek M, et al (2005) Continental insulation, mantle cooling, and the surface area of oceans and continents. *Earth Planet Sci Lett* 234:317–333. <https://doi.org/10.1016/j.epsl.2005.01.038>
- Lerner P, Romanou A, Way M, et al (2025) Obliquity dependence of ocean productivity and atmospheric CO₂ on Earth-like worlds. *Astrophys J* 979(2):234. <https://doi.org/10.3847/1538-4357/ada277>
- Lewis NT, Lambert FH, Boutle IA, et al (2018) The influence of a substellar continent on the climate of a tidally locked exoplanet. *Astrophys J* 854:171. <https://doi.org/10.3847/1538-4357/aaad0a>
- Li Y, Vočadlo L, Sun T, et al (2020) The Earth’s core as a reservoir of water. *Nat Geosci* 13(6):453–458. <https://doi.org/10.1038/s41561-020-0578-1>
- Li J, Liu H, Meng X, et al (2025) Ancient ocean coastal deposits imaged on Mars. *Proc Natl Acad Sci USA* 122(9):e2422213122. <https://doi.org/10.1073/pnas.2422213122>
- Lichtenberg T, Golabek GJ, Burn R, et al (2019) A water budget dichotomy of rocky protoplanets from ²⁶Al-heating. *Nat Astron* 3(4):307–313. <https://doi.org/10.1038/s41550-018-0688-5>. arXiv:1902.04026 [astro-ph, physics:physics]
- Lichtenberg T, Drażkowska J, Schönbächler M, et al (2021) Bifurcation of planetary building blocks during Solar System formation. *Science* 371(6527):365–370. <https://doi.org/10.1126/science.abb3091>
- Lineweaver CH, Chopra A (2012) The habitability of our Earth and other earths: astrophysical, geochemical, geophysical, and biological limits on planet habitability. *Annu Rev Earth Planet Sci* 40(1):597–623
- Lingam M, Loeb A (2018) Implications of tides for life on exoplanets. *Astrobiology* 18(7):967–982. <https://doi.org/10.1089/ast.2017.1718>. arXiv:1707.04594 [astro-ph.EP]
- Lingam M, Loeb A (2019) Dependence of biological activity on the surface water fraction of planets. *Astron J* 157(1):25. <https://doi.org/10.3847/1538-3881/aaf420>. arXiv:1809.09118 [astro-ph.EP]
- Lingam M, Loeb A (2021) Characteristics of aquatic biospheres on temperate planets around Sun-like stars and M dwarfs. *Mon Not R Astron Soc* 503(3):3434–3448. <https://doi.org/10.1093/mnras/stab611>. arXiv:2005.14387 [astro-ph.EP]
- Lingam M, Balbi A, Mahajan SM (2023) A Bayesian analysis of technological intelligence in land and oceans. *Astrophys J* 945(1):23. <https://doi.org/10.3847/1538-4357/acb6fa>. arXiv:2305.05989 [astro-ph.EP]

- Lithgow-Bertelloni C, Silver PG (1998) Dynamic topography, plate driving forces and the African superswell. *Nature* 395(6699):269–272
- Liu T, Jing Z (2024) Hydrogen and silicon are the preferred light elements in Earth’s core. *Commun Earth Environ* 5(1):282
- Liu Z, Fei H, Chen L, et al (2021) Bridgmanite is nearly dry at the top of the lower mantle. *Earth and Planetary Science Letters* 570:117088. <https://doi.org/10.1016/j.epsl.2021.117088>
- Liu S, Moulin A, Jónsson S (2024) Unloading uplift caused by surface processes in New Zealand’s southern Alps. *Geophys Res Lett* 51(15):e2024GL109019. <https://doi.org/10.1029/2024GL109019>
- Lobo AH, Shields AL, Palubski IZ, et al (2023) Terminator habitability: the case for limited water availability on M-dwarf planets. *Astrophys J* 945(2):161. <https://doi.org/10.3847/1538-4357/aca970>
- Lourenço DL, Rozel AB, Ballmer MD, et al (2020) Plutonic-squishy lid: a new global tectonic regime generated by intrusive magmatism on Earth-like planets. *Geochem Geophys Geosyst* 21(4):e2019GC008756
- Lourenço DL, et al (2026) Rocky planets as heat engines. *Space Sci Rev* 226
- Lu W, Yang YN, Long T, et al (2025) Substantial water retained early in Earth’s deep mantle. *Science* 390(6778):1177–1180. <https://doi.org/10.1126/science.adx5883>
- Luo H, Dorn C, Deng J (2024) The interior as the dominant water reservoir in super-Earths and sub-Neptunes. *Nat Astron* 8:1399–1407. <https://doi.org/10.1038/s41550-024-02347-z>
- Lustig-Yaeger J, Meadows VS, Mendoza GT, et al (2018) Detecting ocean glint on exoplanets using multi-phase mapping. *Astron J* 156(6):301. <https://doi.org/10.3847/1538-3881/aaed3a>
- Lustig-Yaeger J, et al (2026) The geoscience and observation of hot rocky worlds. *Space Sci Rev* 222
- Maccone C (2009) SETI, extrasolar planets search and interstellar flight: when are they going to merge? *Acta Astronaut* 64:724–734. <https://doi.org/10.1016/j.actaastro.2008.11.006>
- Macdonald E, Paradise A, Menou K, et al (2022) Climate uncertainties caused by unknown land distribution on habitable M-earths. *Mon Not R Astron Soc* 513(2):2761–2769. <https://doi.org/10.1093/mnras/stac1040>
- Malarewicz V, Beyssac O, Zanda B, et al (2025) Evidence for pre-Noachian granitic rocks on Mars from quartz in meteorite NWA 7533. *Nat Geosci* 1–6. <https://doi.org/10.1038/s41561-025-01653-z>
- Malaska MJ, Radebaugh J, Lopes RMC, et al (2020) Labyrinth terrain on Titan. *Icarus* 344:113764. <https://doi.org/10.1016/j.icarus.2020.113764>
- Malin MC, Edgett KS (1999) Oceans or seas in the Martian northern lowlands: high resolution imaging tests of proposed coastlines. *Geophys Res Lett* 26(19):3049–3052. <https://doi.org/10.1029/1999GL002342>
- Mandt KE, Lustig-Yaeger J, Luspay-Kuti A, et al (2024) A nearly terrestrial D/H for comet 67P/Churyumov-Gerasimenko. *Sci Adv* 10(46):eadp2191. <https://doi.org/10.1126/sciadv.adp2191>
- Marty B (2012) The origins and concentrations of water, carbon, nitrogen and noble gases on Earth. *Earth Planet Sci Lett* 313–314:56–66. <https://doi.org/10.1016/j.epsl.2011.10.040>
- Marzotto E, Hsieh WP, Ishii T, et al (2020) Effect of water on lattice thermal conductivity of ringwoodite and its implications for the thermal evolution of descending slabs. *Geophys Res Lett* 47(13):e2020GL087607
- Maurice M, Dasgupta R, Hassanzadeh P (2024) Volatile atmospheres of lava worlds. *Astron Astrophys.* <https://doi.org/10.1051/0004-6361/202347749>. [arXiv:2405.09284](https://arxiv.org/abs/2405.09284) [astro-ph]
- May R, McLean AR (2007) *Theoretical ecology: principles and applications*, 3rd edn. Oxford University Press, Cambridge
- McGovern PJ, Schubert G (1989) Thermal evolution of the Earth: effects of volatile exchange between atmosphere and interior. *Earth Planet Sci Lett* 96(1–2):27–37
- McGregor NJ, Nimmo F, Gillmann C, et al (2025) Probing the viscosity of Venus’s mantle from dynamic topography at Baltis Vallis. *J Geophys Res Planets* 130(3):e2024JE008581. <https://doi.org/10.1029/2024JE008581>
- McSween HY Jr, Murchie SL, Crisp JA, et al (1999) Chemical, multispectral, and textural constraints on the composition and origin of rocks at the Mars Pathfinder landing site. *J Geophys Res Planets* 104(E4):8679–8715. <https://doi.org/10.1029/98JE02551>
- Melosh HJ (2011) Strength versus gravity. In: Melosh HJ (ed) *Planetary surface processes*. Cambridge planetary science. Cambridge University Press, Cambridge, pp 49–103. <https://doi.org/10.1017/CBO9780511977848.004>
- Mettler JN, Quanz SP, Helled R (2020) Earth as an exoplanet: I. Time variable thermal emission using spatially resolved MODIS data. *Astron J* 160(6):246. <https://doi.org/10.3847/1538-3881/abbc15>. [arXiv:2010.02589](https://arxiv.org/abs/2010.02589) [astro-ph]
- Mibe K, Kanzaki M, Kawamoto T, et al (2007) Second critical endpoint in the peridotite-H₂O system. *Journal of Geophysical Research: Solid Earth* 112(B3). <https://doi.org/10.1029/2005JB004125>
- Michalski JR, Deanne Rogers A, Edwards CS, et al (2024) Diverse volcanism and crustal recycling on early Mars. *Nat Astron* 8(4):456–462. <https://doi.org/10.1038/s41550-023-02191-7>

- Miyazaki Y, Korenaga J (2022a) Inefficient water degassing inhibits ocean formation on rocky planets: an insight from self-consistent mantle degassing models. *Astrobiology* 22(6):713–734. <https://doi.org/10.1089/ast.2021.0126>
- Miyazaki Y, Korenaga J (2022b) A wet heterogeneous mantle creates a habitable world in the Hadean. *Nature* 603(7899):86–90. <https://doi.org/10.1038/s41586-021-04371-9>
- Mojzsis SJ, Harrison TM, Pidgeon RT (2001) Oxygen-isotope evidence from ancient zircons for liquid water at the Earth's surface 4300 Myr ago. *Nature* 409(6817):178–181. <https://doi.org/10.1038/35051557>
- Moore WB, Lenardic A (2015) The efficiency of plate tectonics and nonequilibrium dynamical evolution of planetary mantles. *Geophys Res Lett* 42(21):9255–9260. <https://doi.org/10.1002/2015GL065621>
- Moore WB, Webb AAG (2013) Heat-pipe Earth. *Nature* 501(7468):501–505
- Moore K, Cowan NB, Boukar CÉ (2023) The role of magma oceans in maintaining surface water on rocky planets orbiting M-dwarfs. *Mon Not R Astron Soc* 526:6235–6247. <https://doi.org/10.1093/mnras/stad3138>
- Morbiddelli A, Chambers J, Lunine JJ, et al (2000) Source regions and time scales for the delivery of water to Earth. *Meteoritics & amp. Planet Sci J* 35(6):1309–1320. <https://doi.org/10.1111/j.1945-5100.2000.tb01518.x>
- Morrison D, Jones TJ, Cruikshank DP, et al (1975) The two faces of Iapetus. *Icarus* 24(2):157–171. [https://doi.org/10.1016/0019-1035\(75\)90093-7](https://doi.org/10.1016/0019-1035(75)90093-7)
- Mosenfelder JL, Bureau H, Withers AC (2024) Hydrogen in the deep Earth. *Elements* 20(4):223–228
- Moyen JF, Laurent O (2018) Archaean tectonic systems: a view from igneous rocks. *Lithos* 302–303:99–125. <https://doi.org/10.1016/j.lithos.2017.11.038>
- Mulkidjanian A, Bychkov A, Litrova D, et al (2012) Origin of first cells at terrestrial, anoxic geothermal fields. *Proc Natl Acad Sci USA* 109(14):E821–E830. <https://doi.org/10.1073/pnas.1117774109>
- Murchie SL, Watters TR, Robinson MS, et al (2008) Geology of the Caloris Basin, Mercury: a view from MESSENGER. *Science* 321(5885):73–76. <https://doi.org/10.1126/science.1159261>
- Nakagawa T (2023) Numerical modeling on global-scale mantle water cycle and its impact on the sea-level change. *Earth Planet Sci Lett* 619:118312. <https://doi.org/10.1016/j.epsl.2023.118312>
- Nakayama A, Kodama T, Ikoma M, et al (2019) Runaway climate cooling of ocean planets in the habitable zone: a consequence of seafloor weathering enhanced by melting of high-pressure ice. *Mon Not R Astron Soc* 488:1580–1596. <https://doi.org/10.1093/mnras/stz1812>
- Nance RD (2022) The supercontinent cycle and Earth's long-term climate. *Ann NY Acad Sci* 1515(1):33–49. <https://doi.org/10.1111/nyas.14849>
- Neumann GA, Zuber MT, Wieczorek MA, et al (2004) Crustal structure of Mars from gravity and topography. *J Geophys Res Planets* 109(E8). <https://doi.org/10.1029/2004JE002262>
- Nicholls H, Lichtenberg T, Bower DJ, et al (2024) Magma ocean evolution at arbitrary redox state. <https://doi.org/10.48550/arXiv.2411.19137>. arXiv:2411.19137
- Nimmo F, Primack J, Faber SM, et al (2020) Radiogenic heating and its influence on rocky planet dynamos and habitability. *Astrophys J* 903(2):L37. <https://doi.org/10.3847/2041-8213/abc251>. arXiv:2011.04791
- Noack L, Godolt M, von Paris P, et al (2014) Can the interior structure influence the habitability of a rocky planet? *Planet Space Sci* 98:14–29. <https://doi.org/10.1016/j.pss.2014.01.003>
- Noack L, Höning D, Rivoldini A, et al (2016) Water-rich planets: how habitable is a water layer deeper than on Earth? *Icarus* 277:215–236. <https://doi.org/10.1016/j.icarus.2016.05.009>
- Noack L, Rivoldini A, van Hoolst T (2017) Volcanism and outgassing of stagnant-lid planets: implications for the habitable zone. *Phys Earth Planet Inter* 269:40–57. <https://doi.org/10.1016/j.pepi.2017.05.010>
- Novella D, Demouchy S, Bolfan-Casanova N (2024) Deep hydrogen reservoirs and longevity. *Elements* 20(4):235–240
- Ohtani E (2021) Hydration and dehydration in Earth's interior. *Annu Rev Earth Planet Sci* 49:253–278. <https://doi.org/10.1146/annurev-earth-080320-062509>
- Okuchi T (1997) Hydrogen partitioning into Molten iron at high pressure: implications for Earth's core. *Science* 278(5344):1781–1784. <https://doi.org/10.1126/science.278.5344.1781>
- Olson P, Sharp ZD (2018) Hydrogen and helium ingassing during terrestrial planet accretion. *Earth Planet Sci Lett* 498:418–426. <https://doi.org/10.1016/j.epsl.2018.07.006>
- Olson PL, Sharp ZD (2019) Nebular atmosphere to magma ocean: a model for volatile capture during Earth accretion. *Phys Earth Planet Inter* 294:106294. <https://doi.org/10.1016/j.pepi.2019.106294>
- Olson SL, Jansen M, Abbot DS (2020) Oceanographic considerations for exoplanet life detection. *Astrophys J* 895(1):19. <https://doi.org/10.3847/1538-4357/ab88c9>. arXiv:1909.02928 [astro-ph.EP]
- O'Neil J, Rizo H, Reimink J, et al (2024) Earth's earliest crust. *Elements* 20(3):168–173. <https://doi.org/10.2138/gselements.20.3.168>
- O'Neill C, Lenardic A, Höink T, et al (2013) Mantle convection and outgassing on terrestrial planets. In: *Comparative climatology of terrestrial planets*. University of Arizona Press, Tucson, pp 473–486. https://doi.org/10.2458/azu_uapress_9780816530595-ch019

- O'Reilly TC, Davies GF (1981) Magma transport of heat on Io: a mechanism allowing a thick lithosphere. *Geophys Res Lett* 8:313–316. <https://doi.org/10.1029/GL008i004p00313>
- Ortenzi G, Noack L, Sohl F, et al (2020) Mantle redox state drives outgassing chemistry and atmospheric composition of rocky planets. *Sci Rep* 10(1):1–14
- Owen JE, Shaikhislamov IF, Lammer H, et al (2020) Hydrogen dominated atmospheres on terrestrial mass planets: evidence, origin and evolution. *Space Sci Rev* 216:129. <https://doi.org/10.1007/s11214-020-00756-w>
- Palin RM, Moore JDP, Zhang Z, et al (2021) Mafic Archean continental crust prohibited exhumation of orogenic UHP eclogite. *Geosci Front* 12(5):101225. <https://doi.org/10.1016/j.gsf.2021.101225>
- Parai R, Mukhopadhyay S (2012) How large is the subducted water flux? New constraints on mantle regassing rates. *Earth Planet Sci Lett* 317:318
- Parmentier EM, Head JW (1981) Viscous relaxation of impact craters on icy planetary surfaces: determination of viscosity variation with depth. *Icarus* 47(1):100–111. [https://doi.org/10.1016/0019-1035\(81\)90095-6](https://doi.org/10.1016/0019-1035(81)90095-6)
- Pasek MA, Omran A, Feng T, et al (2022) Serpentinization as a route to liberating phosphorus on habitable worlds. *Geochim Cosmochim Acta* 336:332–340. <https://doi.org/10.1016/j.gca.2022.09.027>
- Pearce BKD, Pudritz RE, Semenov DA, et al (2017) Origin of the RNA world: the fate of nucleobases in warm little ponds. *Proc Natl Acad Sci USA* 114(43):11327–11332. <https://doi.org/10.1073/pnas.1710339114>
- Pekeris CL (1935) Thermal convection in the interior of the Earth. *Geophys J Int* 3:343–367
- Perron JT, Mitrovica JX, Manga M, et al (2007) Evidence for an ancient Martian ocean in the topography of deformed shorelines. *Nature* 447(7146):840–843. <https://doi.org/10.1038/nature05873>
- Peslier AH, Schönbacher M, Busemann H, et al (2017) Water in the Earth's interior: distribution and origin. *Space Sci Rev* 212(1):743–810. <https://doi.org/10.1007/s11214-017-0387-z>
- Pettengill GH, Eliason E, Ford PG, et al (1980) Pioneer Venus Radar results altimetry and surface properties. *J Geophys Res Space Phys* 85(A13):8261–8270. <https://doi.org/10.1029/JA085iA13p08261>
- Phillips BR, Coltice N (2010) Temperature beneath continents as a function of continental cover and convective wavelength. *J Geophys Res, Solid Earth* 115(B4)
- Pierrehumbert RT (2011) A palette of climates for gliese 581g. *Astrophys J* 726:L8. <https://doi.org/10.1088/2041-8205/726/1/L8>
- Pogge Von Strandmann PAE, Jones MT, West AJ, et al (2021) Lithium isotope evidence for enhanced weathering and erosion during the Paleocene-Eocene thermal maximum. *Sci Adv* 7(42):eabh4224. <https://doi.org/10.1126/sciadv.abh4224>
- Rahbek C, Borregaard MK, Colwell RK, et al (2019) Humboldt's enigma: what causes global patterns of mountain biodiversity? *Science* 365(6458):1108–1113. <https://doi.org/10.1126/science.aax0149>
- Rahmstorf S (2002) Ocean circulation and climate during the past 120,000 years. *Nature* 419(6903):207–214. <https://doi.org/10.1038/nature01090>
- Raymond SN, Quinn T, Lunine JI (2004) Making other earths: dynamical simulations of terrestrial planet formation and water delivery. *Icarus* 168:1–17. <https://doi.org/10.1016/j.icarus.2003.11.019>
- Reese CC, Orth CP, Solomatov VS (2011) Impact megadomes and the origin of the Martian crustal dichotomy. *Icarus* 213(2):433–442. <https://doi.org/10.1016/j.icarus.2011.03.028>
- Rey PF, Coltice N (2008) Neoproterozoic lithospheric strengthening and the coupling of Earth's geochemical reservoirs. *Geology* 36(8):635–638
- Rey PF, Coltice N, Flament N (2024) Archean geodynamics underneath weak, flat, and flooded continents. *Elements* 20(3):180–186
- Ricard Y, Richards M, Lithgow-Bertelloni C, et al (1993) A geodynamic model of mantle density heterogeneity. *J Geophys Res, Solid Earth* 98(B12):21895–21909
- Richard G, Monnereau M, Ingrin J (2002) Is the transition zone an empty water reservoir? Inferences from numerical model of mantle dynamics. *Earth Planet Sci Lett* 205(1):37–51. [https://doi.org/10.1016/S0012-821X\(02\)01012-9](https://doi.org/10.1016/S0012-821X(02)01012-9)
- Ringwood AE, Major A (1967) High-pressure reconnaissance investigations in the system Mg₂SiO₄-MgO-H₂O. *Earth Planet Sci Lett* 2:130–133
- Robinson TD, Meadows VS, Crisp D, et al (2011) Earth as an extrasolar planet: Earth model validation using EPOXI Earth observations. *Astrobiology* 11(5):393–408. <https://doi.org/10.1089/ast.2011.0642>
- Robinson TD, Ennico K, Meadows VS, et al (2014) Detection of ocean glint and ozone absorption using LCROSS Earth observations. *Astrophys J* 787(2):171. <https://doi.org/10.1088/0004-637X/787/2/171>. [arXiv:1405.4557 \[astro-ph\]](https://arxiv.org/abs/1405.4557)
- Rosas JC, Korenaga J (2018) Rapid crustal growth and efficient crustal recycling in the early Earth: implications for Hadean and Archean geodynamics. *Earth Planet Sci Lett* 494:42–49. <https://doi.org/10.1016/j.epsl.2018.04.051>
- Rosenzweig ML (1995) *Species diversity in space and time*. Cambridge University Press, Cambridge
- Rudnick RL, Gao S (2003) Composition of the continental crust. *Treatise on Geochemistry* 3:659. <https://doi.org/10.1016/B0-08-043751-6/03016-4>

- Rüpke L, Gaillard F (2024) The geological history of water: from Earth's accretion to the modern deep water cycle. *Elements* 20(4):253–258
- Rushby AJ, Shields AL, Joshi M (2019) The effect of land fraction and host star spectral energy distribution on the planetary albedo of terrestrial worlds. *Astrophys J* 887:29. <https://doi.org/10.3847/1538-4357/ab4da6>
- Russell HN (1906) On the light variations of asteroids and satellites. *Astrophys J* 24:1–18. <https://doi.org/10.1086/141361>
- Russell MJ (2021) The “water problem” (sic), the illusory pond and life's submarine emergence—a review. *Life* 11(5):429. <https://doi.org/10.3390/life11050429>
- Rykaczewski RR, Checkley DM Jr (2008) Influence of ocean winds on the pelagic ecosystem in upwelling regions. *Proc Natl Acad Sci USA* 105(6):1965–1970. <https://doi.org/10.1073/pnas.0711777105>
- Sagan C, Thompson WR, Carlson R, et al (1993) A search for life on Earth from the Galileo spacecraft. *Nature* 365(6448):715–721. <https://doi.org/10.1038/365715a0>
- Salazar AM, Olson SL, Komacek TD, et al (2020) The effect of substellar continent size on ocean dynamics of Proxima Centauri b. *Astrophys J Lett* 896(1):L16. <https://doi.org/10.3847/2041-8213/ab94c1>. arXiv: 2005.14185 [astro-ph.EP]
- Salvador A, Samuel H (2023) Convective outgassing efficiency in planetary magma oceans: insights from computational fluid dynamics. *Icarus* 390:115265. <https://doi.org/10.1016/j.icarus.2022.115265> arXiv: 2209.06199 [astro-ph, physics:physics]
- Salvador A, Massol H, Davaille A, et al (2017) The relative influence of h₂o and co₂ on the primitive surface conditions and evolution of rocky planets. *J Geophys Res Planets* 122(7):1458–1486
- Salvador A, Avice G, Breuer D, et al (2023) Magma ocean, water, and the early atmosphere of Venus. *Space Sci Rev* 219(7):51. <https://doi.org/10.1007/s11214-023-00995-7>
- Sanderson H, Bryson J, Nichols C (2024) Differences in thermal and dynamo histories between carbonaceous and non-carbonaceous achondrites. In: AGU Fall Meeting abstracts, pp DI31A–03
- Sandu C, Lenardic A, McGovern P (2011) The effects of deep water cycling on planetary thermal evolution. *J Geophys Res, Solid Earth* 116(B12). <https://doi.org/10.1029/2011JB008405>
- Sarmiento JL, Gruber N (2006) Ocean biogeochemical dynamics. Princeton University Press, Princeton
- Saurety A, Caracas R, Raymond SN (2025) Impact-induced Vaporization During Accretion of Planetary Bodies. <https://doi.org/10.3847/2041-8213/adb30e>. arXiv:2502.04787
- Schaefer L, Sasselov D (2015) The persistence of oceans on Earth-like planets: insights from the deep-water cycle. *Astrophys J* 801(1):40. <https://doi.org/10.1088/0004-637X/801/1/40>. arXiv:1501.00735
- Scheller EL, Ehlmann BL, Hu R, et al (2021) Long-term drying of Mars by sequestration of ocean-scale volumes of water in the crust. *Science* 372(6537):56–62. <https://doi.org/10.1126/science.abc7717>
- Scherf M, Lammer H, Spross L (2024) Eta-Earth revisited ii: deriving a maximum number of Earth-like habitats in the galactic disk. *Astrobiology* 24(10):e916–e1061. <https://doi.org/10.1089/ast.2023.0076>
- Schlesinger WH, Bernhardt ES (2013) Biogeochemistry: an analysis of global change, 3rd edn. Academic Press, New York
- Schmidt F, Way MJ, Costard F, et al (2022) Circumpolar ocean stability on Mars 3 Gy ago. *Proc Natl Acad Sci USA* 119(4):e2112930118. <https://doi.org/10.1073/pnas.2112930118>
- Schneider J, Silk J, Vakili F (2022) OWL-Moon: very high resolution spectropolarimetric interferometry and imaging from the Moon: exoplanets to cosmology. *Exp Astron* 54(2–3):1351–1357. <https://doi.org/10.1007/s10686-022-09868-3>. arXiv:2208.05971 [astro-ph.IM]
- Schreiber Maia J, Plesa AC, Tosi N, et al (2024) The viscosity structure of Venus' Mantle: models and observations. In: AGU Fall Meeting abstracts, pp DI44A–04
- Schultz RA, Frey HV (1990) A new survey of multiring impact basins on Mars. *J Geophys Res, Solid Earth* 95(B9):14175–14189. <https://doi.org/10.1029/JB095iB09p14175>
- Schulze-Makuch D, Heller R, Guinan E (2020) In search for a planet better than Earth: top contenders for a superhabitable world. *Astrobiology* 20(12):1394–1404. <https://doi.org/10.1089/ast.2019.2161>
- Schwartz JC, Sekowski C, Haggard HM, et al (2016) Inferring planetary obliquity using rotational and orbital photometry. *Mon Not R Astron Soc* 457:926–938. <https://doi.org/10.1093/mnras/stw068>
- Seager S, Turner E, Schafer J, et al (2005) Vegetation's red edge: a possible spectroscopic biosignature of extraterrestrial plants. *Astrobiology* 5(3):372–390. <https://doi.org/10.1089/ast.2005.5.372>
- Seales J, Lenardic A (2020) Deep water cycling and the multi-stage cooling of the Earth. *Geochem Geophys Geosyst* 21(10):e09106. <https://doi.org/10.1029/2020GC009106>
- Shah O, Alibert Y, Helled R, et al (2021) Internal water storage capacity of terrestrial planets and the effect of hydration on the M-R relation. *Astron Astrophys* 646:A162. <https://doi.org/10.1051/0004-6361/202038839>
- Sharp ZD (2017) Nebular ingassing as a source of volatiles to the Terrestrial planets. *Chem Geol* 448:137–150. <https://doi.org/10.1016/j.chemgeo.2016.11.018>










- Sharp ZD, McCubbin FM, Shearer CK (2013) A hydrogen-based oxidation mechanism relevant to planetary formation. *Earth Planet Sci Lett* 380:88–97. <https://doi.org/10.1016/j.epsl.2013.08.015>
- Shields AL, Meadows VS, Bitz CM, et al (2013) The effect of host star spectral energy distribution and ice-albedo feedback on the climate of extrasolar planets. *Astrobiology* 13:715–739 <https://doi.org/10.1089/ast.2012.0961>
- Sigman DM, Hain MP (2012) The biological productivity of the ocean. *Nature Education Knowledge* 3(6):1–16
- Simpson F (2017) Bayesian evidence for the prevalence of waterworlds. *Mon Not R Astron Soc* 468:2803–2815. <https://doi.org/10.1093/mnras/stx516>
- Sizova E, Gerya T, Stüwe K, et al (2015) Generation of felsic crust in the Archean: a geodynamic modeling perspective. *Precambrian Res* 271:198–224. <https://doi.org/10.1016/j.precamres.2015.10.005>
- Solomatov VS (1993) Parameterization of temperature- and stress-dependent viscosity convection and the thermal evolution of Venus. In: Stone DB, Runcorn SK (eds) *Flow and creep in the Solar System: observations, modeling and theory*. NATO ASI Series. Springer, Dordrecht, pp 131–145. https://doi.org/10.1007/978-94-015-8206-3_10
- Solomon SC (1977) The relationship between crustal tectonics and internal evolution in the moon and Mercury. *Phys Earth Planet Inter* 15:135–145. [https://doi.org/10.1016/0031-9201\(77\)90026-7](https://doi.org/10.1016/0031-9201(77)90026-7)
- Sossi PA, Tollan PME, Badro J, et al (2023) Solubility of water in peridotite liquids and the prevalence of steam atmospheres on rocky planets. *Earth Planet Sci Lett* 601:117894. <https://doi.org/10.1016/j.epsl.2022.117894>
- Spaargaren RJ, Ballmer MD, Bower DJ, et al (2020) The influence of bulk composition on the long-term interior-atmosphere evolution of terrestrial exoplanets. *Astron Astrophys*, 643:A44. <https://doi.org/10.1051/0004-6361/202037632>
- Spiegel DS, Raymond SN, Dressing CD, et al (2010) Generalized Milankovitch cycles and long-term climatic habitability. *Astrophys J* 721(2):1308–1318. <https://doi.org/10.1088/0004-637X/721/2/1308>
- Spohn T, et al (2026) Exo-geoscience perspectives beyond habitability. *Space Sci Rev* 222. <https://doi.org/10.1007/s11214-026-01265-y>
- Stein M, Ben-Avraham Z (2015) Mechanisms of continental growth. In: Stevenson D, Schubert G (eds) *Treatise on geophysics*, 2nd edn. vol 9. Elsevier, New York, pp 173–199
- Steinberger B, Conrad CP, Tutu AO, et al (2019) On the amplitude of dynamic topography at spherical harmonic degree two. *Tectonophysics* 760:221–228
- Stern RJ, Gerya TV (2024) The importance of continents, oceans and plate tectonics for the evolution of complex life: implications for finding extraterrestrial civilizations. *Sci Rep* 14:8552. <https://doi.org/10.1038/s41598-024-54700-x>
- Stern R, Gerya T, Tackley P (2023) A tectonic manifesto. *Persp Earth Space Sci* 4(1):e2023CN000214. <https://doi.org/10.1029/2023CN000214>
- Stolper E, Walker D, Hager BH, et al (1981) Melt segregation from partially Molten source regions: the importance of melt density and source region size. *J Geophys Res, Solid Earth* 86(B7):6261–6271. <https://doi.org/10.1029/JB086iB07p06261>
- Straume EO, Steinberger B, Becker TW, et al (2024) Impact of mantle convection and dynamic topography on the Cenozoic paleogeography of Central Eurasia and the West Siberian Seaway. *Earth Planet Sci Lett* 630:118615. <https://doi.org/10.1016/j.epsl.2024.118615>
- Syverson DD, Reinhard CT, Isson TT, et al (2021) Nutrient supply to planetary biospheres from anoxic weathering of mafic Oceanic crust. *Geophys Res Lett* 48(19):e94442. <https://doi.org/10.1029/2021GL094442>. [arXiv:2002.07667](https://arxiv.org/abs/2002.07667) [astro-ph.EP]
- Szathmáry E, Maynard Smith J (1995) The major evolutionary transitions. *Nature* 374(6519):227–232. <https://doi.org/10.1038/374227a0>
- Tackley PJ (2023) Tectono-convective modes on Earth and other terrestrial bodies. In: *Dynamics of plate tectonics and mantle convection*, pp 159–180
- Tagawa S, Sakamoto N, Hirose K, et al (2021) Experimental evidence for hydrogen incorporation into Earth's core. *Nat Commun* 12(1):1–8. <https://doi.org/10.1038/s41467-021-22035-0>
- Tang M, Chen K, Rudnick RL (2016) Archean upper crust transition from mafic to felsic marks the onset of plate tectonics. *Science* 351(6271):372–375. <https://doi.org/10.1126/science.aad5513>
- Teinturier L, Vieira N, Jacquet E, et al (2022) Mapping the Surface of Partially Cloudy Exoplanets is Hard. [arXiv:2201.00825](https://arxiv.org/abs/2201.00825) [astro-ph]
- Thackeray CW, Hall A (2019) An emergent constraint on future Arctic sea-ice albedo feedback. *Nat Clim Change* 9(12):972–978. <https://doi.org/10.1038/s41558-019-0619-1>
- Tian F, Ida S (2015) Water contents of Earth-mass planets around M dwarfs. *Nat Geosci* 8:177–180. <https://doi.org/10.1038/ngeo2372>
- Tikoo SM, Elkins-Tanton LT (2017) The fate of water within Earth and super-Earths and implications for plate tectonics. *Philos Trans R Soc A, Math Phys Eng Sci* 375(2094):20150394. <https://doi.org/10.1098/rsta.2015.0394>

- Tosi N, Grott M, Plesa AC, et al (2013) Thermochemical evolution of Mercury's interior. *J Geophys Res Planets* 118(12):2474–2487. <https://doi.org/10.1002/jgre.20168>
- Tosi N, Godolt M, Stracke B, et al (2017) The habitability of a stagnant-lid Earth. *Astron Astrophys* 605:A71. <https://doi.org/10.1051/0004-6361/201730728>
- Tschauner O, Huang S, Greenberg E, et al (2018) Ice-vii inclusions in diamonds: evidence for aqueous fluid in Earth's deep mantle. *Science* 359(6380):1136–1139
- Turbet M, Leconte J, Selsis F, et al (2016) The habitability of Proxima Centauri b - II. Possible climates and observability. *Astron Astrophys* 596:A112. <https://doi.org/10.1051/0004-6361/201629577>
- Turbet M, Bolmont E, Chaverot G, et al (2021) Day–night cloud asymmetry prevents early oceans on Venus but not on Earth. *Nature* 598(7880):276–280. <https://doi.org/10.1038/s41586-021-03873-w>
- Turyshv SG (2018) Direct multipixel images of an exo-Earth with a solar gravitational lens telescope. *J Br Interplanet Soc* 71:361–368. <https://doi.org/10.48550/arXiv.1802.08421>. arXiv:1802.08421 [astro-ph.IM]
- Turyshv SG, Toth VT (2017) Diffraction of electromagnetic waves in the gravitational field of the Sun. *Phys Rev D* 96(2):024008. <https://doi.org/10.1103/PhysRevD.96.024008>. arXiv:1704.06824 [gr-qc]
- Turyshv SG, Toth VT (2022) Resolved imaging of exoplanets with the solar gravitational lens. *Mon Not R Astron Soc* 515(4):6122–6132. <https://doi.org/10.1093/mnras/stac2130>. arXiv:2204.04866 [astro-ph.EP]
- Turyshv SG, Toth VT (2023) Imaging faint sources with the extended solar gravitational lens. *Phys Rev D* 107(10):104063. <https://doi.org/10.1103/PhysRevD.107.104063>. arXiv:2301.07495 [astro-ph.IM]
- Tyrrell T (1999) The relative influences of nitrogen and phosphorus on Oceanic primary production. *Nature* 400(6744):525–531. <https://doi.org/10.1038/22941>
- Unterborn CT, Foley BJ, Desch SJ, et al (2022) Mantle degassing lifetimes through galactic time and the maximum age stagnant-lid rocky exoplanets can support temperate climates. *Astrophys J Lett* 930(1):L6
- Van Keken PE, Hacker BR, Syracuse EM, et al (2011) Subduction factory: 4. Depth-dependent flux of h₂O from subducting slabs worldwide. *J Geophys Res, Solid Earth* 116(B1)
- Van Kranendonk MJ, Baumgartner R, Djokic T, et al (2021) Elements for the origin of life on land: a deep-time perspective from the Pilbara Craton of western Australia. *Astrobiology* 21(1):39–59. <https://doi.org/10.1089/ast.2019.2107>
- Vezenin A, Chugunov AV, Sobolev AV, et al (2025) Growth of continental crust and lithosphere subduction in the Hadean revealed by geochemistry and geodynamics. *Nat Commun* 16(1):3850. <https://doi.org/10.1038/s41467-025-59024-6>
- Wade J, Dyck B, Palin RM, et al (2017) The divergent fates of primitive hydrospheric water on Earth and Mars. *Nature* 552(7685):391–394. <https://doi.org/10.1038/nature25031>
- Wade J, Byrne DJ, Ballentine CJ, et al (2021) Temporal variation of planetary iron as a driver of evolution. *Proc Natl Acad Sci USA* 118:e2109865118. <https://doi.org/10.1073/pnas.2109865118>
- Walbecq A, Samuel H, Limare A (2025) The effect of out-of-equilibrium outgassing on the cooling of planetary magma oceans. *Icarus* 434:116513. <https://doi.org/10.1016/j.icarus.2025.116513>
- Walker J, Hayes P, Kasting J (1981) A negative feedback mechanism for the long-term stabilization of Earth's surface temperature. *J Geophys Res* 86:9776–9782. <https://doi.org/10.1029/JC086iC10p09776>
- Walsh JE, Fetterer F, Scott Stewart J, et al (2017) A database for depicting Arctic sea ice variations back to 1850. *Geogr Rev* 107(1):89–107. <https://doi.org/10.1111/j.1931-0846.2016.12195.x>
- Walton CR, Ringley JK, Lipp A, et al (2024) Cosmic dust fertilization of glacial prebiotic chemistry on early Earth. *Nat Astron* 8(5):556–566. <https://doi.org/10.1038/s41550-024-02212-z>
- Watanabe Y, Tajika E (2021) Atmospheric oxygenation of the early Earth and Earth-like planets driven by competition between land and seafloor weathering. *Earth Planets Space* 73(1):188. <https://doi.org/10.1186/s40623-021-01527-9>
- Way MJ (2025) TRAPPIST-1 d: exo-Venus, exo-Earth, or exo-dead? *Astrophys J Lett* 980(1):L7. <https://doi.org/10.3847/2041-8213/adace0>
- Way MJ, Anthony, Del Genio D (2020) Venusian habitable climate scenarios: modeling Venus through time and applications to slowly rotating Venus-like exoplanets. *J Geophys Res: Planets* 125:e2019JE006276. <https://doi.org/10.1029/2019JE006276>
- Way MJ, Davies HS, Duarte JC, et al (2021) The climates of Earth's next supercontinent: effects of tectonics, rotation rate, and insolation. *Geochem Geophys Geosyst* 22(8):e2021GC009983. <https://doi.org/10.1029/2021GC009983>
- Westall F, Brack A, Fairén AG, et al (2023a) Setting the geological scene for the origin of life and continuing open questions about its emergence. *Front Astron Space Sci* 9:1095701. <https://doi.org/10.3389/fspas.2022.1095701>
- Westall F, Höning D, Avicé G, et al (2023b) The habitability of Venus. *Space Sci Rev* 219:17. <https://doi.org/10.1007/s11214-023-00960-4>

- Wilhelms DE, Squyres SW (1984) The Martian hemispheric dichotomy may be due to a giant impact. *Nature* 309(5964):138–140. <https://doi.org/10.1038/309138a0>
- Williams Q (2007) Water, the solid Earth, and the atmosphere: the genesis and effects of a wet surface on a mostly dry planet. In: Stevenson D, Schubert G (eds) *Treatise on geophysics*, vol 9. Elsevier, New York, pp 121–143
- Wolf L, Huismans RS, Rouby D, et al (2022) Links between faulting, topography, and sediment production during continental rifting: insights from coupled surface process, thermomechanical modeling. *J Geophys Res, Solid Earth* 127(3):e2021JB023490. <https://doi.org/10.1029/2021JB023490>
- Worsley TR, Nance D, Moody JB (1984) Global tectonics and eustasy for the past 2 billion years. *Mar Geol* 58(3):373–400. [https://doi.org/10.1016/0025-3227\(84\)90209-3](https://doi.org/10.1016/0025-3227(84)90209-3)
- Wu B, Dong J, Wang Y, et al (2024) A probable ancient nearshore zone in southern Utopia on Mars unveiled from observations at the Zhurong landing area. *Sci Rep* 14(1):24389. <https://doi.org/10.1038/s41598-024-75507-w>
- Yamane M, Yokoyama Y, Abe-Ouchi A, et al (2015) Exposure age and ice-sheet model constraints on Pliocene East Antarctic ice sheet dynamics. *Nat Commun* 6(1):7016. <https://doi.org/10.1038/ncomms8016>
- Yang J, Liu Y, Hu Y, et al (2014) Water trapping on tidally locked terrestrial planets requires special conditions. *Astrophys J* 796:L22. <https://doi.org/10.1088/2041-8205/796/2/L22>
- Young ED, Shahar A, Schlichting HE (2023) Earth shaped by primordial H₂ atmospheres. *Nature* 616(7956):306–311. <https://doi.org/10.1038/s41586-023-05823-0>
- Zaffos A, Finnegan S, Peters SE (2017) Plate tectonic regulation of global marine animal diversity. *Proc Natl Acad Sci USA* 114(22):5653–5658. <https://doi.org/10.1073/pnas.1702297114>
- Zahnle KJ, Kasting JF, Pollack JB (1988) Evolution of a steam atmosphere during Earth's accretion. *Icarus* 74:62–97. [https://doi.org/10.1016/0019-1035\(88\)90031-0](https://doi.org/10.1016/0019-1035(88)90031-0)
- Zhang X, Jiao Z, Zhao C, et al (2022) Review of land surface albedo: variance characteristics, climate effect and management strategy. *Remote Sens* 14(6):1382. <https://doi.org/10.3390/rs14061382>
- Zhao Z, Liu Y, Li W, et al (2021) Climate change of over 20 °C induced by continental movement on a synchronously rotating exoplanet. *Astrophys J Lett* 910(1):L8. <https://doi.org/10.3847/2041-8213/abebe6>
- Zhao M, Mills BJW, Poulton SW, et al (2024) Drivers of the global phosphorus cycle over geological time. *Nat Rev, Earth Environ* 5(12):873–889. <https://doi.org/10.1038/s43017-024-00603-4>
- Zuber MT, Smith DE, Lemoine FG, et al (1994) The shape and internal structure of the moon from the clementine mission. *Science* 266(5192):1839–1843. <https://doi.org/10.1126/science.266.5192.1839>

Publisher's Note Springer Nature remains neutral with regard to jurisdictional claims in published maps and institutional affiliations.

Authors and Affiliations

Claire Marie Guimond¹  · Tilman Spohn²  · Svetlana Berdyugina³  · Paul K. Byrne⁴  · Nicolas Coltice⁵  · Donald M. Glaser^{6,7}  · Manasvi Lingam⁸  · Charles H. Lineweaver⁹  · Peter A. Cawood¹⁰ 

✉ C.M. Guimond
claire.guimond@physics.ox.ac.uk

¹ Atmospheric, Oceanic, and Planetary Physics, University of Oxford, Parks Rd, Oxford OX1 3PU, UK

² Institute of Space Research, German Aerospace Center (DLR), Rutherfordstr. 2, Berlin, 12489, Germany

³ Istituto ricerche solari Aldo e Cele Daccó (IRSOL), Faculty of Informatics, Università della Svizzera italiana, Via Patocchi 57, Locarno, 6605, Switzerland

⁴ Department of Earth, Environmental, and Planetary Sciences, Washington University in St. Louis, 1 Brookings Drive, St. Louis, MO, 63130, USA

⁵ UMR GéoAzur, Université Côte d'Azur, 250 rue Albert Einstein, Valbonne, France

- ⁶ Goddard Institute for Space Studies, 2880 Broadway, New York, NY, 10025, USA
- ⁷ Blue Marble Space Institute of Science, 600 1st Avenue, Seattle, WA, 98104, USA
- ⁸ Department of Aerospace, Physics and Space Sciences, Florida Institute of Technology, 150 W. University Blvd., Melbourne, FL, 32901, USA
- ⁹ Research School of Astronomy & Astrophysics, Australian National University, Canberra, 2600, Australia
- ¹⁰ School of Earth, Atmosphere & Environment, Monash University, 9 Rainforest Walk, Clayton, Victoria, 3800, Australia